

A STUDY OF BIOAEROSOL SAMPLING CYCLONES

A Thesis

by

BRANDON WAYNE MONCLA

Submitted to the Office of Graduate Studies of
Texas A&M University
in partial fulfillment of the requirements for the degree of

MASTER OF SCIENCE

December 2004

Major Subject: Mechanical Engineering

A STUDY OF BIOAEROSOL SAMPLING CYCLONES

A Thesis

by

BRANDON WAYNE MONCLA

Submitted to Texas A&M University
in partial fulfillment of the requirements
for the degree of

MASTER OF SCIENCE

Approved as to style and content by:

Andrew R. McFarland
(Chair of Committee)

Dennis O'Neal
(Member)

Yassin A. Hassan
(Member)

Dennis O'Neal
(Head of Department)

December 2004

Major Subject: Mechanical Engineering

ABSTRACT

A Study of Bioaerosol Sampling Cyclones. (December 2004)

Brandon Wayne Moncla, B.S., Texas A&M University

Chair of Advisory Committee: Dr. Andrew R. McFarland

A wetted wall cyclone using an airblast atomizer upstream of the inlet was designed as an improvement of a wetted wall cyclone developed by White et al. in 1975, which uses liquid injection through a port on the wall of the cyclone inlet. In the course of this project, many changes to different aspects of the White-type cyclone design and operation were considered. These included inlet configuration, liquid delivery, porous media, surface finishes and coatings, outlet skimmer design, and cyclone body length.

The final airblast atomizer cyclone (AAC) design considered has an aerosol-to-hydrosol collection efficiency cut-point of 1.6 μm with collection efficiencies at 2 and 3 μm of 65% and 85%, respectively. The efficiency reported for the White-type cyclone for single *Bacillus globigii* spores that have a particle size of about 1 μm was approximately 81.8%. The aerosol-to-aerosol transmission efficiency for the AAC configuration was found to be approximately 50% for 1 μm diameter particles as compared with 70 – 100% for the White-type cyclone.

A time response test was performed in which the White-type (ca. 2003) cyclone had an initial response of 3 minutes for a condition where there was no liquid carryover through the cyclone outlet and 8 minutes on average with hydrosol carryover. The decay response of the White-type cyclone was 1.25 minutes for non-liquid carryover conditions. The AAC had an initial response of 2.75 minutes and a decay response of 2.5 minutes. The shortened version of the AAC had an initial response of 1.5 minutes and a decay response of 1.25 minutes. There was no liquid carryover observed for any tests of this cyclone configuration.

Power consumption tests were performed comparing pressure drops across different variations of White-type cyclones (circa 2003 and 1999) including a variation with an electrical discharge machined (EDM) inlet profile, that reduces the pressure drop at a nominal air flowrate of 780 L/min from 18 inH₂O for the basic White-type cyclone (ca. 2003) to 16 inH₂O with use of the EDM inlet. Two different variations of White-type cyclones were found to have pressure drops of 25 inH₂O and 18 inH₂O at an air flowrate of 780 L/min.

DEDICATION

This work is dedicated my wife, Amber. Her love and support are my inspiration for all that I do. To my parents, Wayne and Lynda Moncla, for their encouragement and love that set the foundation from which I build my life. To my brother, Aaron, who has encouraged me with our shared love and respect for each other. And to Shorts, my cat, who always greeted me at the door after a late night of work.

ACKNOWLEDGEMENTS

Funding for this study was provided by the U.S. Army Research, Development and Engineering Command, Edgewood Center, under contracts DAAD13-02-C-0064 and DAAD13-03-C-0050. Dr. Jerold R. Bottiger was the Project Technical Officer for Edgewood.

I would like to thank the members of my committee for their time and guidance, and the members of the Aerosol Technology Laboratory, especially Carlos Ortiz, Dr. John Haglund, Manpreet Phull, and John Vaughan.

TABLE OF CONTENTS

	Page
ABSTRACT	iii
DEDICATION	v
ACKNOWLEDGEMENTS	vi
TABLE OF CONTENTS	vii
LIST OF FIGURES.....	viii
LIST OF TABLES	x
NOMENCLATURE.....	xi
INTRODUCTION.....	1
DESIGN AND THEORY	3
EXPERIMENTAL PROCEDURE	17
Polystyrene Latex Sphere Techniques	17
Master Solution Method.....	19
Aerosol-to-Hydrosol and Aerosol-to-Aerosol Performance	23
Time Response of the Cyclone.....	26
Power Consumption of the Cyclone.....	29
RESULTS AND DISCUSSION	33
Aerosol-to-Hydrosol and Aerosol-to-Aerosol Performance	33
Time Response of the Cyclone.....	41
Power Consumption of the Cyclone.....	43
SUMMARY AND CONCLUSIONS.....	47
Aerosol-to-Hydrosol and Aerosol-to-Aerosol Performance	47
Time Response of the Cyclone.....	48
Power Consumption of the Cyclone.....	48
Final Remarks	48
RECOMMENDATIONS FOR FUTURE WORK.....	50
REFERENCES	51
APPENDIX	52
VITA	55

LIST OF FIGURES

	Page
Figure 1. Schematic of cyclone developed by White et al. as tested by Richardson (ca. 2002).	3
Figure 2. Water injection hole on inlet of White-type cyclone (ca. 2003).	4
Figure 3. Sectioned view of transpirated wall cyclone (TWC).	5
Figure 4. Sectioned view of tangential transpirated wall cyclone (TTWC).	6
Figure 5. SEM photo of sintered metal surface.	7
Figure 6. SEM photo of 1 bar rated ceramic surface.	8
Figure 7. SEM photo of 0.5 bar rated ceramic surface.	9
Figure 8. Sectioned view of airblast atomizer cyclone (AAC).	11
Figure 9. Outlet skimmers used with cyclones.	12
Figure 10. Acrylic AAC with uncoated outlet skimmer modeled after White-type cyclone (ca. 2002).	13
Figure 11. Acrylic AAC with outlet skimmer modeled after White-type cyclone (ca. 2003).	14
Figure 12. Sectioned view of the shortened AAC.	15
Figure 13. Outlet skimmer tested with shortened acrylic AAC.	16
Figure 14. Comparison of fluorometric analysis for ethyl acetate and isopropyl alcohol.	19
Figure 15. Normalized output of 24-jet Collison nebulizer over time for different particle sizes.	21
Figure 16. Comparison of normalized nebulizer output for master solution method and mixing individual suspensions for each test.	22
Figure 17. Schematic of test apparatus for aerosol performance evaluation of cyclones.	24
Figure 18. Schematic of test apparatus for power consumption test.	31
Figure 19. Aerosol-to-hydrosol collection efficiency of the White-type cyclone (ca. 2003).	34

	Page
Figure 20. Aerosol-to-aerosol collection efficiency of the White-type cyclone (ca. 2003).....	35
Figure 21. Aerosol-to-hydrosol collection efficiency of AAC with aluminum outlet skimmer.....	36
Figure 22. Aerosol-to-hydrosol collection efficiency of AAC with coated, hydrophobic outlet skimmer.....	37
Figure 23. Aerosol-to aerosol collection efficiency of AAC with aluminum outlet skimmer.....	38
Figure 24. Aerosol-to-aerosol collection efficiency of AAC with coated, hydrophobic outlet skimmer.....	39
Figure 25. Aerosol-to-hydrosol collection efficiency of shortened AAC with grooved outlet skimmer.....	40
Figure 26. Time response of the White-type cyclone (ca. 2003).....	41
Figure 27. Time response of AAC with hydrophobic coating on outlet skimmer....	42
Figure 28. Time response of shortened AAC with grooved outlet skimmer.....	43
Figure 29. Power consumption vs. air flowrate through wetted wall cyclones using blower models 116634, 117418, and 119104.....	44
Figure 30. Differential pressure across cyclones with flow straightener in place using blower models 11634, 117418, and 119104.....	45
Figure 31. Comparison of differential pressure measurements taken on each cyclone at the outlet skimmer pressure tap.	46

LIST OF TABLES

	Page
Table 1. Aerosol-to-hydrosol collection efficiencies of cyclones.....	52
Table 2. Aerosol-to-aerosol collection efficiencies of cyclones.	53
Table 3. Recovered wall losses from cyclones.....	54
Table 4. Time response of cyclones.	54

NOMENCLATURE

A	coefficient
B	coefficient
C	concentration
$C_{aerosol}$	concentration of aerosol sample
$C_{corrected}$	concentration of sample corrected for normalized volume of water collected
$C_{hydrosol}$	concentration of hydrosol sample
$C_{reference}$	concentration of reference sample
$C_{wallloss}$	concentration of wall loss sample
ΔP_{4-6}	differential pressure across points 4 and 6 on power measurement test
F	fraction of full scale response
F_{water}	normalized correction factor for volume of water collected
η	efficiency of blower
η_{AA}	aerosol-to-aerosol collection efficiency
η_{AH}	aerosol-to-hydrosol collection efficiency
$\bar{\eta}_{AH}$	average aerosol-to-hydrosol collection efficiency
$m_{initial}$	initial mass of ethyl acetate sample
m_{final}	final mass of ethyl acetate sample
P_1	pressure measured at point 1 on power measurement test
P_{std}	atmospheric pressure
$Power$	power consumed by blower
$Power_{ideal}$	ideal power required by blower
Q	air flowrate
$Q_{standard}$	air flowrate as measured at standard atmospheric conditions
R	fluorometric reading
$\rho_{ethylacetate}$	density of ethyl acetate
t	time
T_1	temperature measured at point 1 on power measurement test

T_{std}	temperature of ambient air
V	volume of ethyl acetate
$V_{initial}$	initial volume of ethyl acetate
V_{water_i}	volume of water collected for individual sample
\bar{V}_{water}	average volume of water collected over all samples
WL	wall loss

INTRODUCTION

White et al. (1975) developed a cyclone for collection of bacterial cells in large volumes of air. The cyclone (see figure on page 3) has a tangential air inlet and an axial airflow layout. Liquid, at a flowrate of about 1.5 mL/min is injected through the wall of the inlet, and then flows into the body of the cyclone where the liquid continuously washes the walls. The liquid follows the air towards the air exhaust port, where it is then skimmed from the flow field by use of a ring that has a somewhat smaller diameter than the cyclone body. Liquid that flows into the gap between the ring and the cyclone body is aspirated from the system by a liquid pump. Air flow through the system is on the order of 1000 L/min. It is desirable that the cyclone efficiently collect particles in the size range of 1 to 10 μm aerodynamic diameter, which is a range of interest for bioaerosols.

The purpose of this project is to explore possible improvements to the White-type cyclone that will reduce its pressure drop, reduce power consumption, and increase the aerosol-to-liquid collection efficiency. Some of the requirements of a cyclone system are that it must be transportable, and it must have low power consumption.

White et al. (1975) presented the aerosol-to-liquid collection efficiency of the cyclone for a number of organisms and for different collection liquids. They determined the aerosol-to-hydrosol efficiency was 81.8% for aerosols comprised of single *Bacillus globigii* cells when the liquid was distilled water plus a surfactant Tween 80 (Fisher Scientific, Fair Lawn, NJ). They used an All-Glass Impinger (AGI) to establish the reference aerosol concentration, and that device was later shown to have an efficiency of 60% for 1 μm particles (Willeke et al. 1998), which implies the actual aerosol-to-hydrosol efficiency for the experiments of White et al. is approximately 50%. White also measured the fractional efficiency (aerosol-to-aerosol collection efficiency) for particles in the size range of 0.5 to 5 μm , and noted that the efficiency was essentially

This thesis follows the style and format of *Aerosol Science and Technology*.

100% for particles larger than 2.3 μm and was 70% for 0.5 μm aerosol particles.

With respect to the question of why there is a difference between the aerosol-to-hydrosol and fractional efficiencies, the answer lies in the fact that collected aerosol particles may adhere to the internal walls of the cyclone and transport tubing rather than be carried by the flow. Reduction of these wall losses is an important part of any effort to improve the performance of a White-type cyclone.

DESIGN AND THEORY

The first White-type cyclone (ca. 2002) made available for this study had been used in experiments involving sampling of postal dust (Richardson, 2003). This unit had six water entry ports equally spaced across the side of the inlet area (Figure 1). Richardson observed that the volume of liquid collected varied with the amount of background material in the air flow such as paper fibers and dust. A second White-type cyclone (ca. 2003), which had only one water injection port (Figure 2), was also used in this study. This cyclone was part of a stand-alone unit.

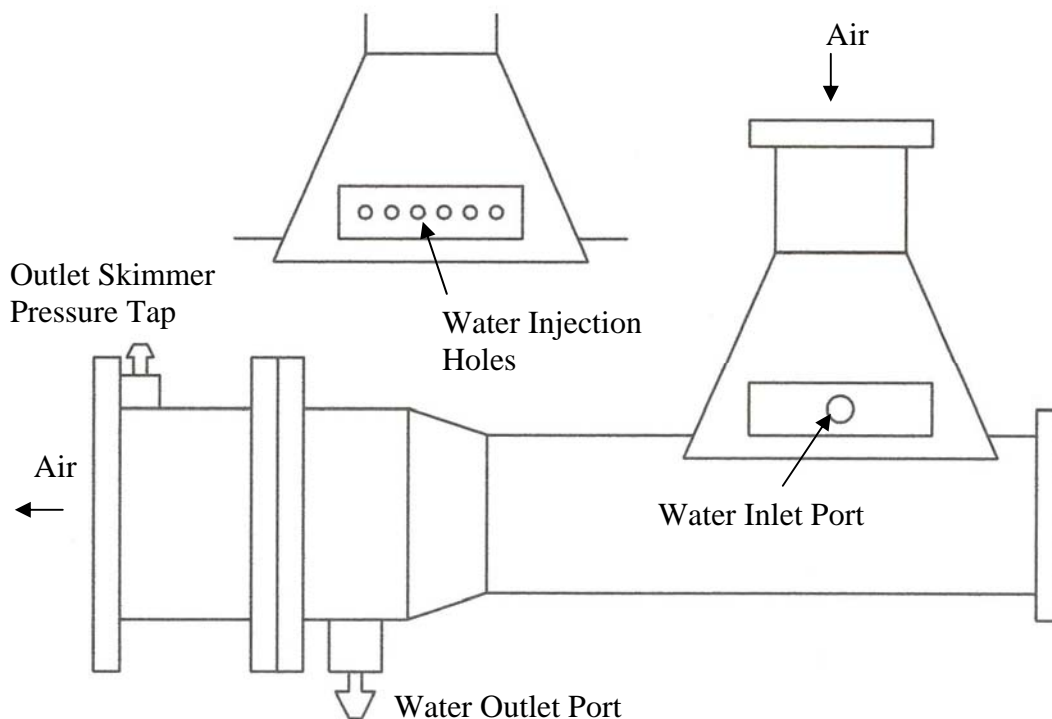


Figure 1. Schematic of cyclone developed by White et al. as tested by Richardson (ca. 2002).

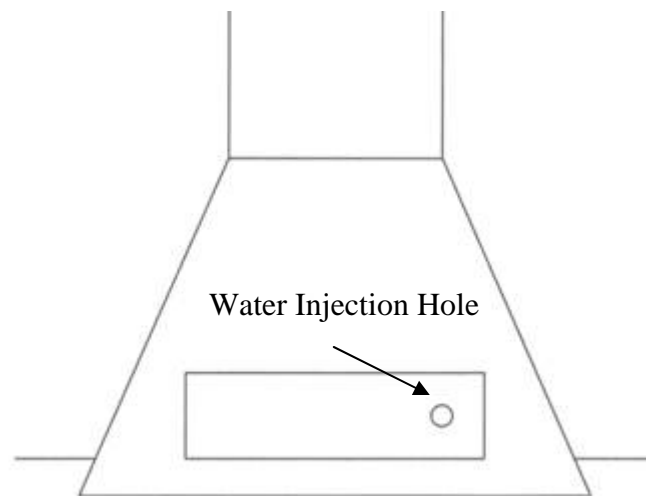


Figure 2. Water injection hole on inlet of White-type cyclone (ca. 2003).

The surface finish on the interior of the White-type cyclones has been improved from a machined finish to a polished finish. The surface was either mechanically polished or electro-polished. The outlet skimmer has been modified with an extension to the leading edge of the outlet skimmer. Evidence of water bypassing the outlet skimmer was present on the stand-alone unit in the form of corrosion on the blower.

It should be noted that on both White-type cyclones, the tapped holes that fasten the water injection manifold over the water injection holes are drilled and tapped through with straight threads. This was found to be a source of an air leak, and in the case of the stand-alone unit, the screws protruded through the holes and across the airflow in the cyclone inlet. Prior to testing, shorter screws were replaced and the threads sealed with silicone.

Using the White-type cyclones as a base-case of study, several cyclone designs and components were evaluated including inlet configuration, liquid delivery, porous media, surface finishes and coatings, outlet skimmer, and cyclone body length. With the exception of the shortened cyclone, the interior dimensions of the cyclones were the same as those of the White-type cyclone.

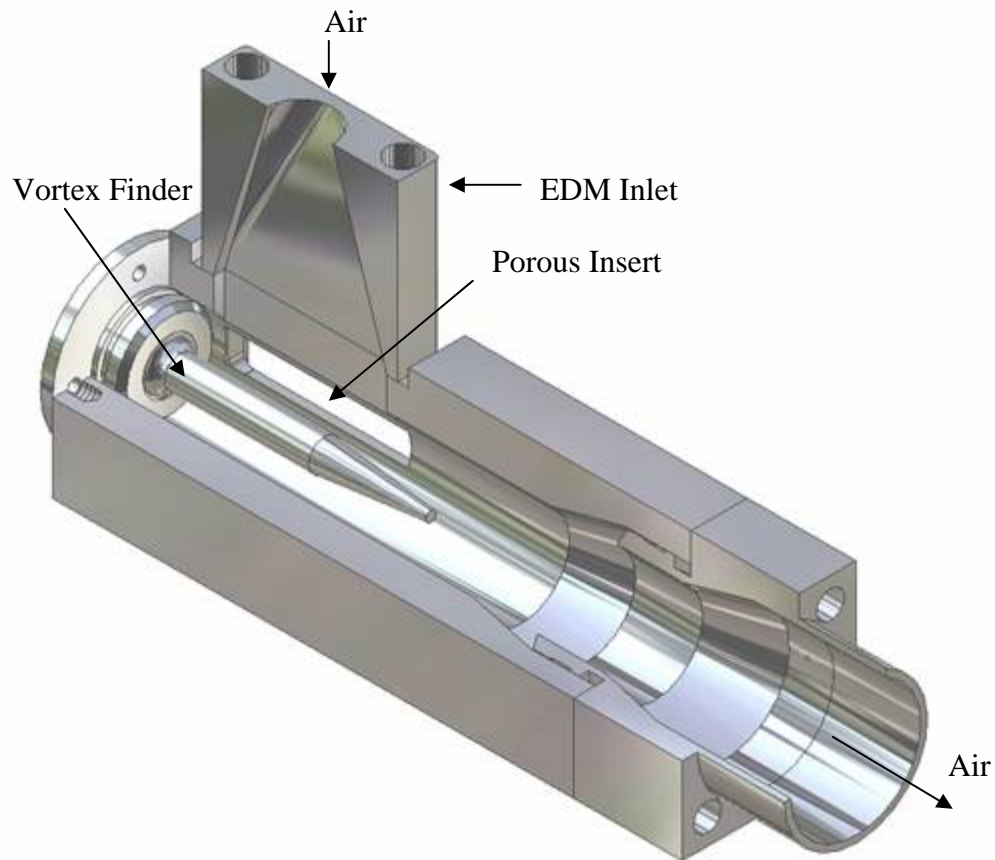


Figure 3. Sectioned view of transpirated wall cyclone (TWC).

This study started with a transpirated wall cyclone (TWC), shown in Figure 3. The TWC had an electrical discharge machined (EDM) inlet which was similar to the White-type cyclone inlet. This inlet changed from a 19.05 mm (0.750 inch) diameter hole to a 6.858 mm x 50.8 mm (0.270 inch x 2.000 inch) rectangular slot over a length of 50.8 mm (2.000 inches). The transpirated surface was made of sintered stainless steel sheet metal (Mott Corporation, Farmington, CT).

Poor aerosol-to-hydrosol collection efficiencies drove a change that resulted in rotating the transpirated surface 19 degrees such that it was tangent to the body of the cyclone and directly below the inlet area where the majority of the particles impact.

This cyclone is referred to as the tangential transpirated wall cyclone (TTWC) and is shown in Figure 4.

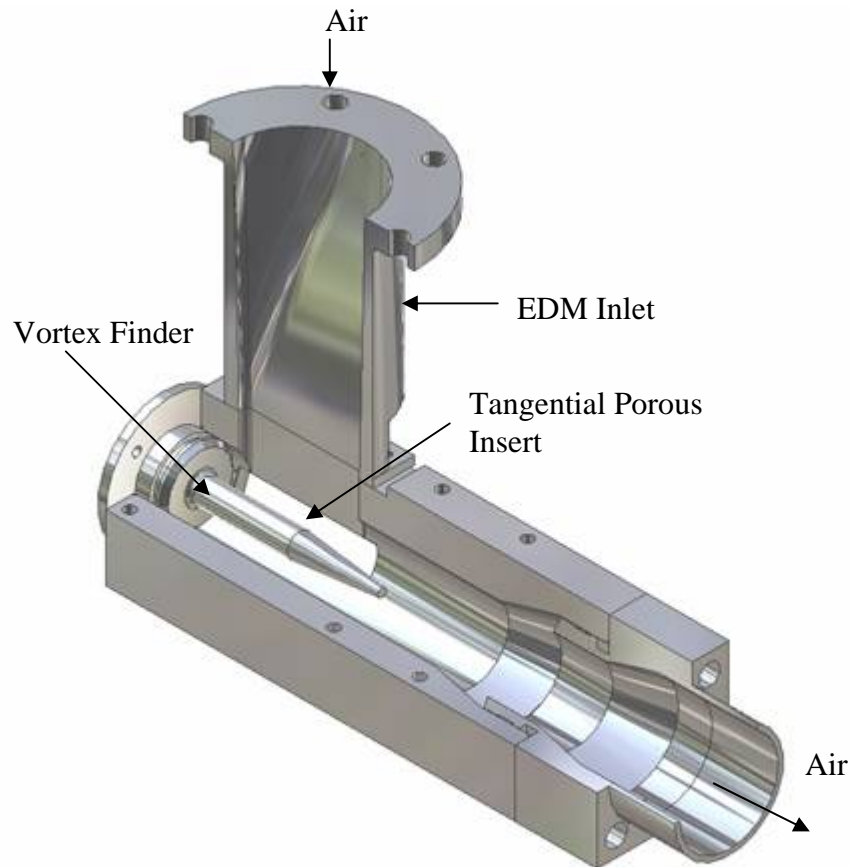


Figure 4. Sectioned view of tangential transpirated wall cyclone (TTWC).

A new EDM inlet configuration was also created for the TTWC cyclone. The inlet progressed from a 50.8 mm (2.000 inch) diameter hole to a 6.35 mm x 46.228 mm (0.250 inch x 1.820 inch) rectangular slot. This change was made because the cross-sectional area decreased with this design, accelerating the air flow. The inlet shape used in conjunction with the White-type cyclone serves to decelerate the incoming air flow, as

the cross-sectional area increases. The 19.05 mm (0.750 inch) diameter also creates a flow constriction.

Different transpired surfaces were evaluated. The sintered metal plates were not producing good aerosol-to-hydrosol efficiencies (less than 40%), and upon visual observations, it was found that only a small part of the surface along the bottom was wetted. As the water flowed from this surface to the wall of the cyclone, it was influenced by machining marks at the interface of the porous plate and the cyclone body. To create better wetting across the porous insert, other materials and designs were tested. Two porous ceramics (SoilMoisture, Inc., Santa Barbara, CA) were ordered and compared to the sintered metal surface using scanning electron microscopy (SEM). The two porous ceramics were rated at pressure drops of 0.5 bar and 1.0 bar. The photos are shown below in Figures 5 through 7.

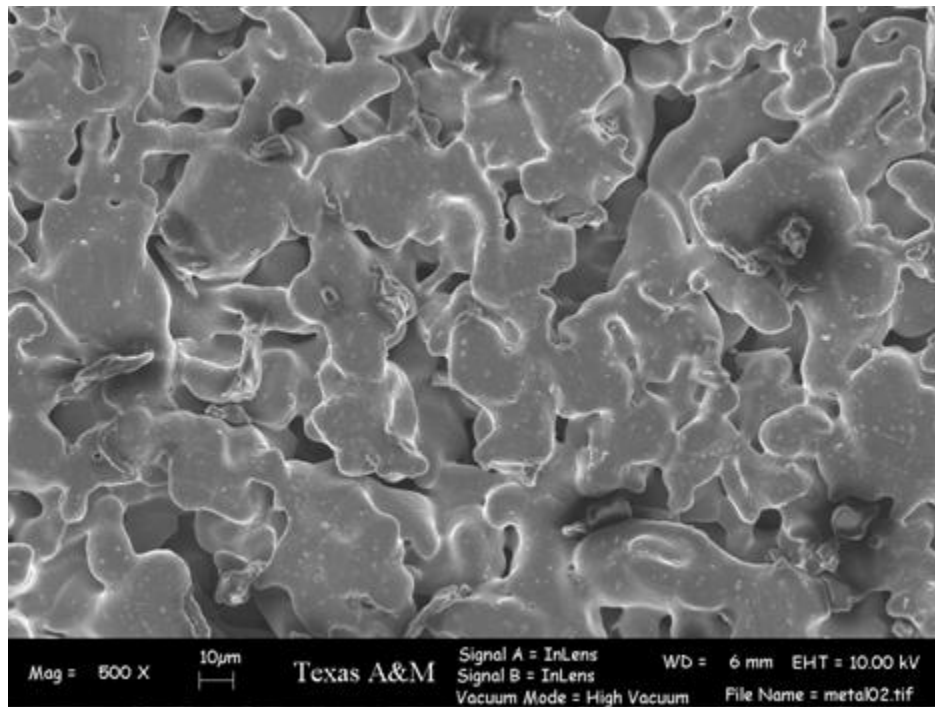


Figure 5. SEM photo of sintered metal surface.

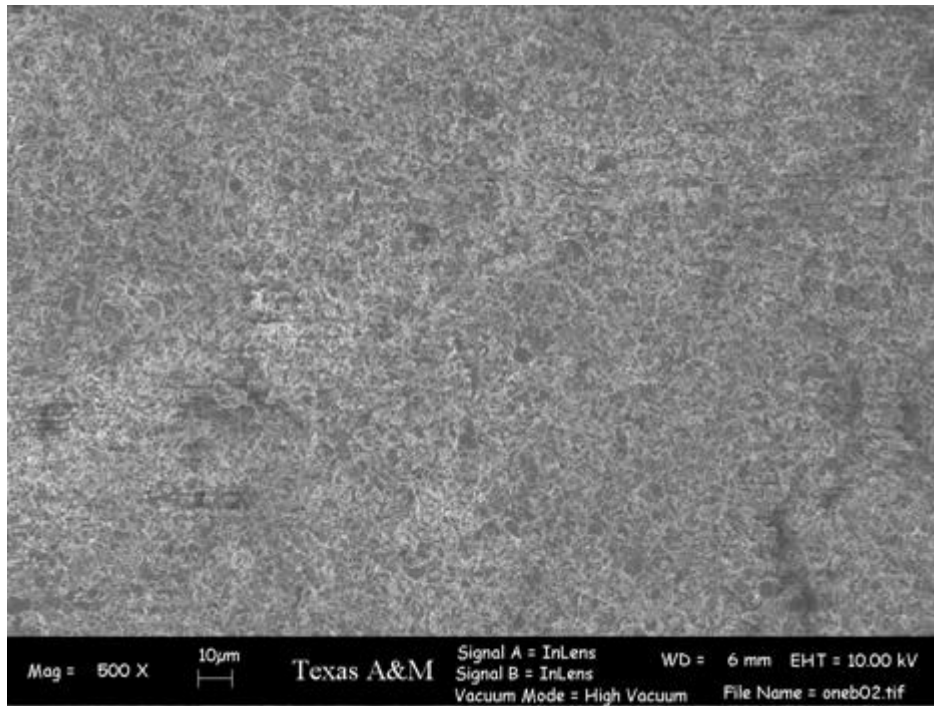


Figure 6. SEM photo of 1 bar rated ceramic surface.

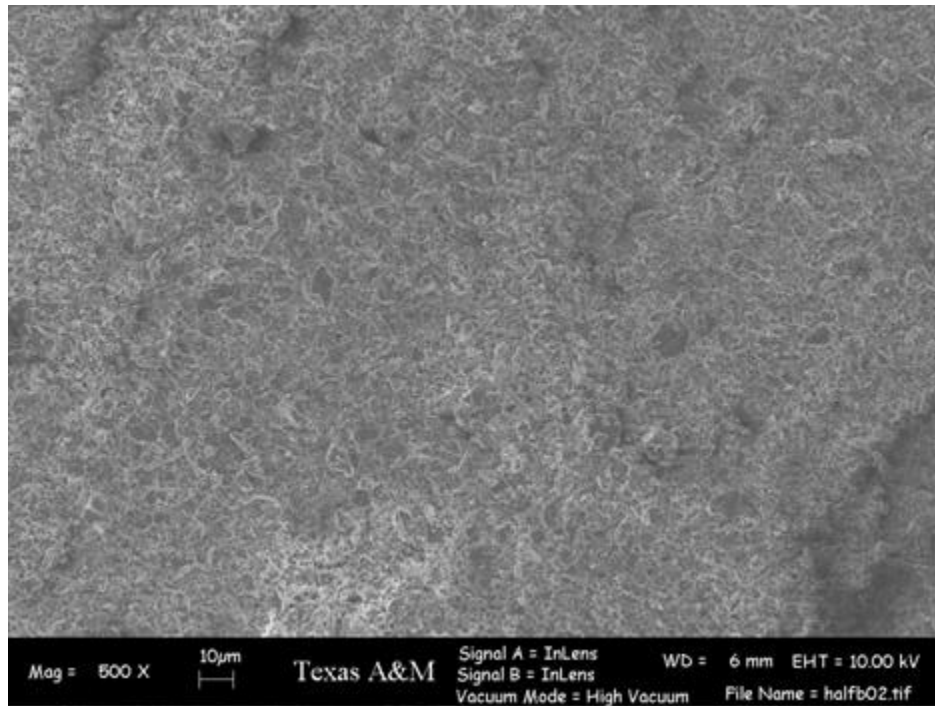


Figure 7. SEM photo of 0.5 bar rated ceramic surface.

The sintered metal has a much rougher surface than that of the ceramics. The liquid film has a much harder time evenly coating a surface of the sintered metal texture. A solid plate was machined with 0.3429 mm (0.0135 inch) holes drilled in a pattern over it. It turned out that there was little pressure drop across this plate and the water only poured through some of the bottom holes. Again, this did not coat the area of interest. In order to correct for the lack of pressure drop across the plate, another solid plate was drilled using a laser and ten 0.0508 mm (0.002 inch) holes were evenly spaced across it (Precision Microfab, Arnold, MD). Visual observations showed that, although most of the water came out of each hole evenly, the interface at the plate and the body of the cyclone continued to disrupt the flow.

Following the White-type cyclone (ca. 2003), the TTWC cyclone was electro-polished (Fin-Tech, Houston, TX) to improve the surface quality. Other surface coatings were investigated to aid in directing hydrosol flow to the outlet skimmer without liquid carryover, and improving surface-wetting capabilities. The body of the cyclone was

coated with a hydrophilic layer (Hydromer, Somerville, NJ). This material is used in the medical industry for items such as catheters, and it had been shown to have an excellent resistance to biological media adhering to it (John et al, 1995). The polystyrene latex particles used in testing proved to have an affinity to the hydrophilic coating which reduced the aerosol-to-hydrosol collection efficiency. No other tests were run with this coating, but it may be of interest to try airborne bacterial media given its resistance to the adherence of biological agents. The vortex finder and the outlet skimmer had a hydrophobic coating of Parylene N applied (Advanced Coatings, Rancho Cucamonga, CA) to prevent water from remaining on these surfaces.

After working with transpired surfaces and coatings, observations of both water movement across the body and poor porous material performance resulted in a change of the introduction of water to the system. An airblast atomizer was placed upstream of the cyclone (airblast atomizer cyclone, AAC) as shown in Figure 8. The porous insert was also removed such that the interior of the body more closely resembles that of the White-type cyclone. A rough estimate based on Ingebo and Foster's equation for cross current breakup in an airblast atomizer results in a 43 μm mean drop size (Lefebvre, 1989). The validity of the estimate is tempered by the fact that in the atomizer used in this study, the air and water flows are not perpendicular to each other.

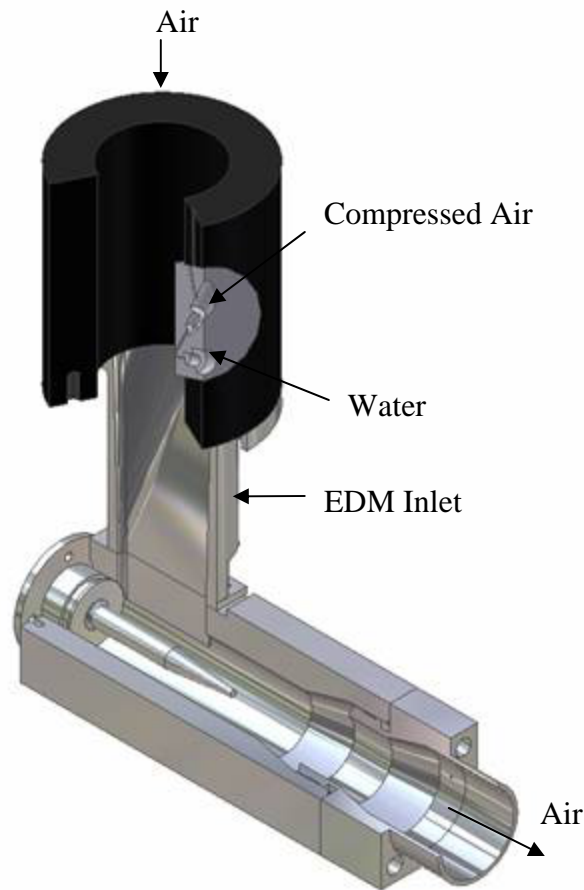
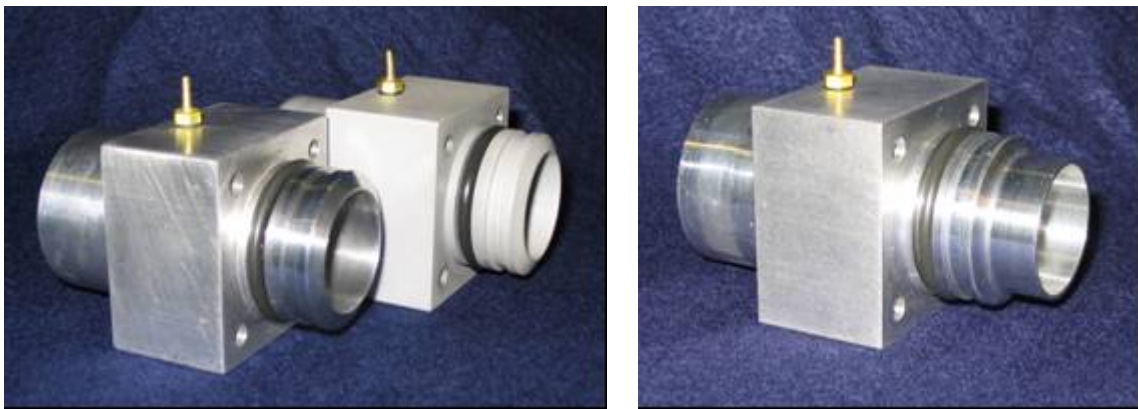


Figure 8. Sectioned view of airblast atomizer cyclone (AAC).

Acrylic versions of the airblast atomizer cyclone were created so that the wetting action and behavior of the cyclones could be seen in real-time test scenarios. This showed that the airblast atomizer produced an excellent wetting affect across the entire entrance region to the cyclone.

Important insight was gained from observing the acrylic cyclones, the action of the skimmer, and the skimmer's ability to effectively remove water from the body of the cyclone. The two types of skimmers used throughout the majority of the work in this report were modeled after two skimmers received with White-type cyclones. See Figure 9 below. The water was unable to pass the first edge of the skimmer easily and began to accumulate just upstream of the skimmer, where the air flow produced a high-velocity,

swirling region in the water. By not removing the hydrosol immediately from the body of the cyclone, it allows for liquid carryover to occur more readily. The slightest bump can “short circuit” the water past the outlet skimmer. Once carryover starts it does not stop. The difference between the two types of outlet skimmers was the location of the residual water circulation. See Figures 10 and 11.



(a)

(b)

Figure 9. Outlet skimmers used with cyclones. (a) Uncoated outlet skimmer and outlet skimmer with hydrophobic coating modeled after first White-type cyclone received. (b) Outlet skimmer with extension modeled after cyclone from stand-alone unit.

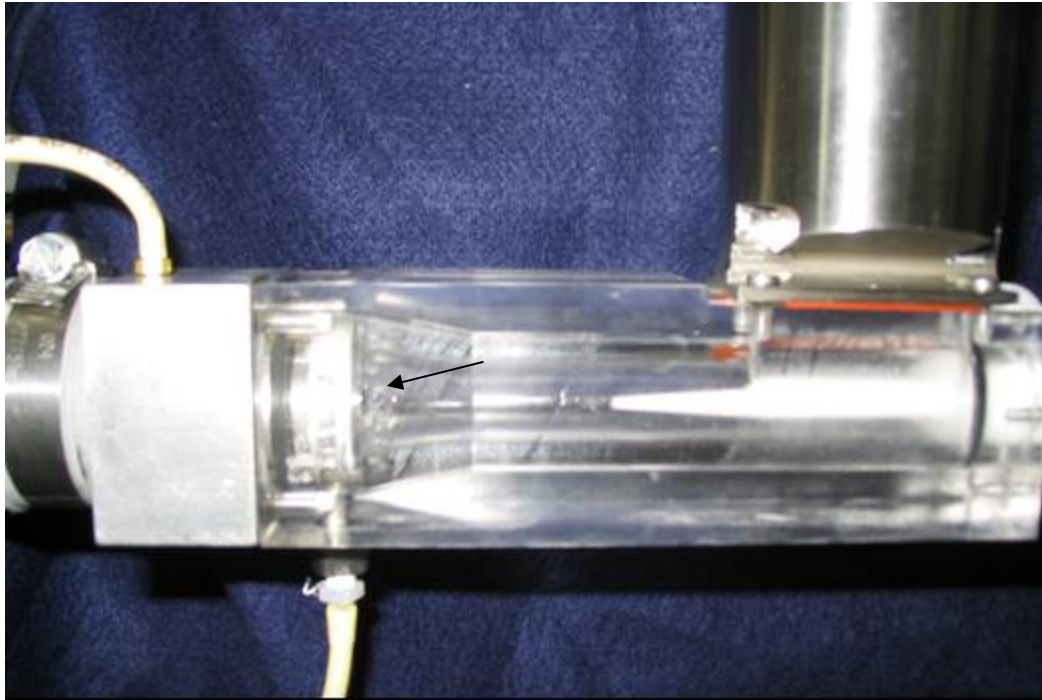


Figure 10. Acrylic AAC with uncoated outlet skimmer modeled after White-type cyclone (ca. 2002). The arrow indicates the recirculation area of the hydrosol.



Figure 11. Acrylic AAC with outlet skimmer modeled after White-type cyclone (ca. 2003). The arrow indicates the recirculation area.

A shortened version of the AAC was produced for testing to see if the time constant could be reduced. It is pictured in Figure 12. Both Delrin and acrylic versions were made of the shortened AAC. The acrylic model allowed for observations of performance of different outlet skimmers. An outlet skimmer similar to the one in Figure 13 was used. Eight grooves were placed along the leading edge to allow for the hydrosol to pass by easier. Although some liquid carryover was observed, the occurrences were less frequent.

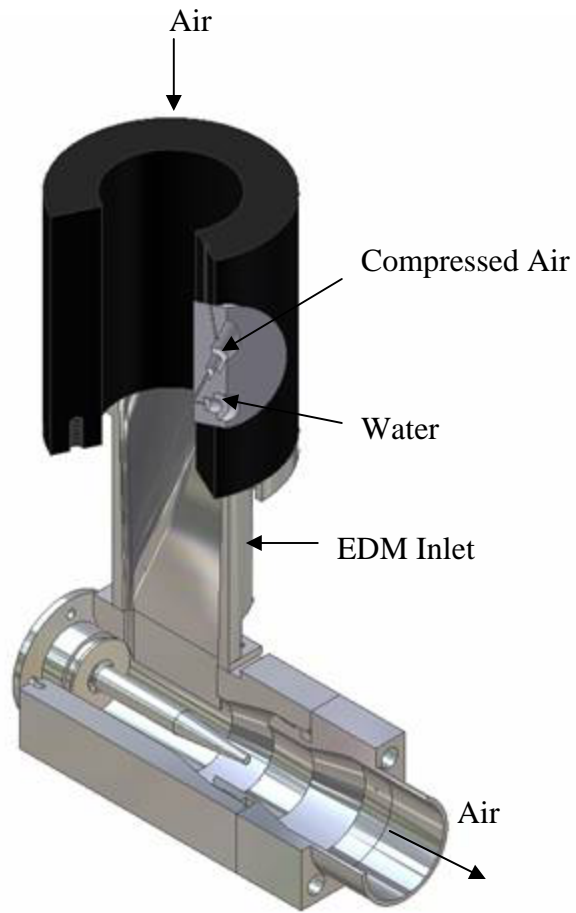


Figure 12. Sectioned view of the shortened AAC.

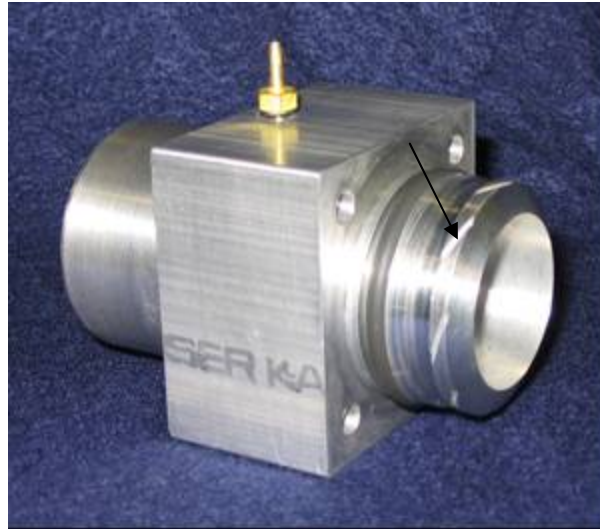


Figure 13. Outlet skimmer tested with shortened acrylic AAC. The arrow indicates one of eight grooves around the leading edge.

The results of the design and evaluation process lead to the need to verify the test apparatus used by reproducing the results of the White-type cyclone (White et al. 1975), and then the development of improvements to the cyclone itself. The airblast atomizer affixed upstream of an EDM inlet was selected as the direction to search, and the uncoated outlet skimmer and the outlet skimmer with the hydrophobic coating would also be reviewed. The shortened AAC would be tested for improvements to the time response of the cyclone. The evaluation procedures follow.

EXPERIMENTAL PROCEDURE

Polystyrene Latex Sphere Techniques

Polystyrene latex (PSL) particles are used to simulate monodisperse aerosol suspensions for testing aerosol sampling equipment and systems. These particles are generally collected on glass fiber or polycarbonate membrane filters and analyzed through fluorometric analysis and optical methods. Fluorescent tracers in the PSL particles allow for the use of these procedures when illuminated at the excitation wavelength. Initially the PSL particles were removed from the filters for fluorometric analysis by submerging the filters in a solution of isopropyl alcohol and ultrasonicing them for a few minutes. The isopropyl alcohol solution containing the suspended particles from the filter was then analyzed with the fluorometer. A manufacturer of PSL particles, Polysciences (Warrington, PA), suggested that ethyl acetate be used to dissolve the PSL particles and fluorescent dye and then subsequently analyze the solution. This method was used by Sioutas, Koutrakis, and Burton (1994). The procedure used to verify this method for use in this test and compare it with the use of an isopropyl alcohol suspension is discussed.

To test these procedures, a solution of distilled water with 0.1% Tween 20 surfactant (Fisher Scientific, Fair Lawn, NJ) was used for the wash liquid and introduction to the polycarbonate membrane filter. To check this method, a suspension of concentrated 0.83 μm PSL from the supplier (Duke Scientific, Palo Alto, CA) was diluted by adding one drop of the PSL to the 0.1% Tween 20 solution. To test for sensitivity of this method, 1 mL of this PSL suspension is then diluted with 10 mL of the 0.1% Tween 20 solution. 1 mL of this solution (1:11) is then diluted once again with another 10 mL of 0.1% Tween 20 (1:101). All of these solutions are shaken to ensure proper mixing. Ultrasonication was not used as it proved to destroy the polycarbonate membrane filters, creating a cloudy sample, and this disturbed the fluorometric analysis.

Four separate 5 mL samples of the 0.1% Tween 20 solution without PSL were first filtered on separate 0.6 μm polycarbonate membrane filters (Isopore, Millipore, 0.6

μm DTTP). Five mL of the undiluted PSL/Tween 20 suspension were then filtered. Four filters were created in this manner. Likewise, eight 5 mL samples of the 1:11 and 1:101 suspensions are used to create eight more filters.

The filters for the background samples and each dilution of the PSL solution were then divided such that two filters were submersed in 10 mL of ethyl acetate and two in 10 mL of isopropyl alcohol. The filters are then stirred and shaken. The results of the fluorometric analysis are given.

A plot of the normalized fluorometric reading versus the concentration of each sample is shown below (Figure 14). Both methods of analysis appear to be linear in nature. However, the isopropyl alcohol gives readings that are much alike for both the 1:11 and 1:101 dilutions. It should also be noted that the readings for the isopropyl suspension are set on the highest gain of the fluorometer (1000X) (Turner Model 450, Mountain View, CA).

This experiment compared the methods of using ethyl acetate and isopropyl alcohol to perform fluorometric analysis on PSL particles. The concern with the filter wash method is that not all particles on the filter will be re-suspended in the isopropyl alcohol solution. By using ethyl acetate, which dissolves the PSL particles, the fluorescent dye is released from the particles and mixes as a solution with the ethyl acetate. The experiment shows that using ethyl acetate is comparable to isopropyl alcohol. Ethyl acetate produces a sensitive, linear, and repeatable method for measuring the fluorescent emissions of PSL particles.

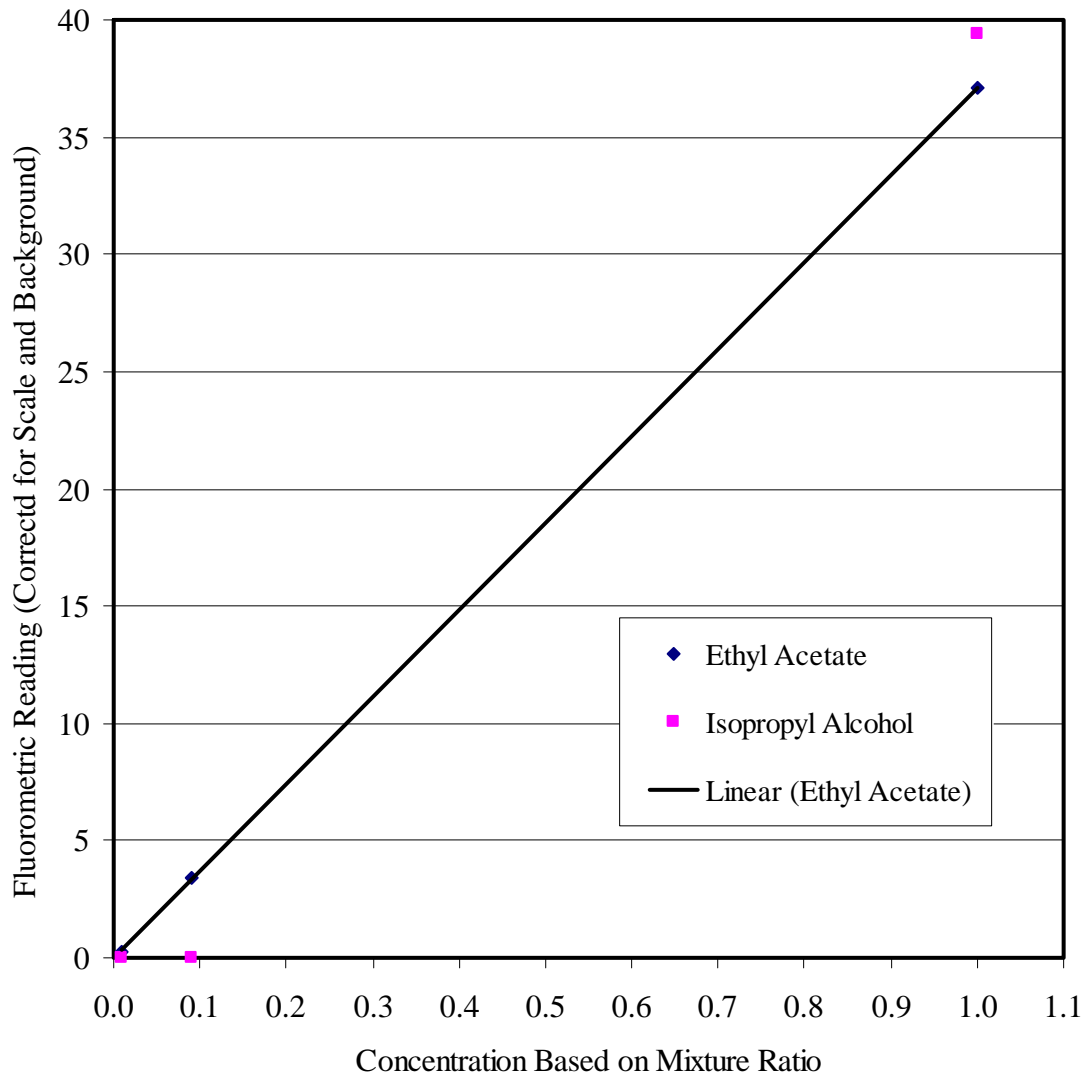


Figure 14. Comparison of fluorometric analysis for ethyl acetate and isopropyl alcohol.

Master Solution Method

The amount of PSL suspended in distilled water is limited by the concentration of PSL doublets in the aerosol, which is caused by two (or more) PSL particles occupying the same water droplet. This doublet no longer behaves as a particle of the

same size. For the Collison nebulizer used in this study (Model CN60, BGI, Inc., Waltham, MA) the limiting concentration is about 10^9 particles/mL (May, 1973).

The 24-jet Collison nebulizer holds enough PSL suspension to run for 45 minutes without adjusting the height of the jets. For shorter tests, it was desired to mix an individual suspension in the nebulizer jar, and use it for multiple runs and only change the suspension after one total hour of testing. Because there was a change in the concentration of individual suspensions for different hourly runs, a new method was developed in which for every test the nebulizer was rinsed and a fresh suspension was added. To insure that the concentration of each of these suspensions remained constant, a large batch of PSL suspension was made, from which each new test suspension was drawn. The large batch is referred to as the “master solution.”

The change of PSL hydrosol concentration with time is shown in Figure 15, which presents the normalized concentration of PSL as a function of time as output by the 24-jet nebulizer. The four particle sizes used in the tests are shown. These outputs represent an average of multiple runs, each from the same master solution. There are two $2\ \mu\text{m}$ runs plotted which show the average outputs for two different master solutions. This shows that two different master solutions vary by less than 7%.

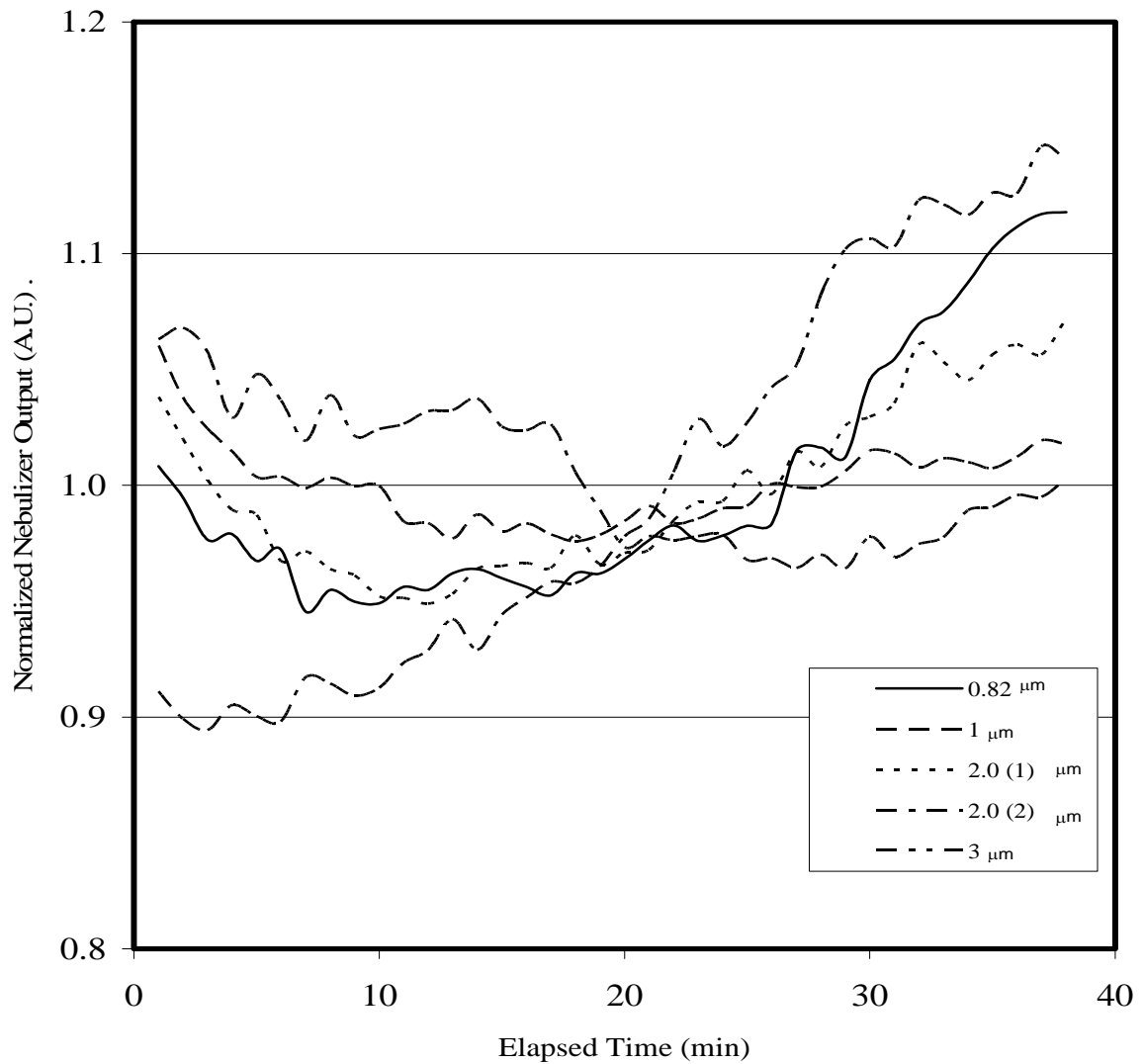


Figure 15. Normalized output of 24-jet Collison nebulizer over time for different particle sizes.

Prior to receiving the 24-jet nebulizer, a test was run with a 6-jet Collison nebulizer to compare the master solution method with the method of mixing a new suspension for each run. A master solution of 0.93 μm PSL was mixed. Five 30 minute runs were made in which the PSL suspension was changed out each time from the same

master solution. These were compared to six samples taken for 1 hour, mixing a new suspension for each run. Plots of the normalized nebulizer PSL output are shown in Figure 16.

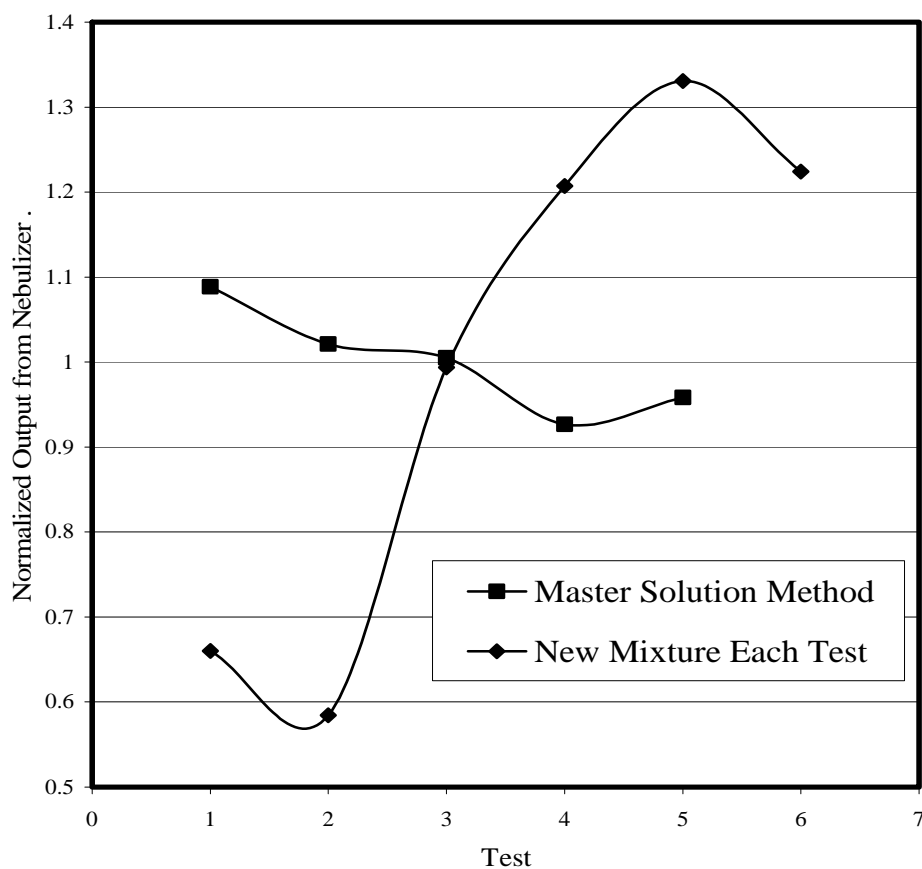


Figure 16. Comparison of normalized nebulizer output for master solution method and mixing individual suspensions for each test.

The master solution method gave an output within $\pm 10\%$ each time. Mixing an individual solution each time varied by $\pm 40\%$. The master solution method is used for all runs with PSL reported.

Aerosol-to-Hydrosol and Aerosol-to-Aerosol Performance

Aerosol-to-aerosol and aerosol-to-hydrosol efficiencies of the multiple cyclone configurations were measured for comparison. Of most importance were the AAC, shortened AAC, and the White-type cyclone (ca. 2003). The air flowrate was set at 780 L/min, and the hydrosol flowrate was set such that 1 mL/min was retrieved. For the spray atomizer configuration, 1.4 mL/min was input to attain 1 mL/min at the outlet skimmer when there was no liquid carryover. The test apparatus is shown in Figure 17.

A 24-jet Collison nebulizer (Models CN60 (24 Jet), BGI, Inc., Waltham, MA) was used to generate monodisperse polystyrene latex particles (PSL) (Duke Scientific, Palo Alto, CA) of various sizes. The air pressure to the nebulizer was set at 138 kPa (20 psi). HEPA-filtered drying air was mixed with the spray from the nebulizer. The aerosol was then passed through a mixer (Blender Products, Inc. Denver, CO), and then through a flow straightener, a 1 L/min sample of aerosol was extracted from the flow for analysis with an aerodynamic particle sizer (APS) (Model 3321, TSI, Shoreview, MN). If there was a change in aerosol concentration or composition (i.e., the fraction of doublets), it would be detected with the APS.

The air flow then passes through either the cyclone or reference filter which, were sequentially exposed to the aerosol. A 203 mm x 254 mm (8 inch x 10 inch) glass fiber filter (Type A/E, Pall, East Hills, NY) was placed at the outlet of the cyclone to collect particles that were transmitted through the cyclone. The air was then passed through a laminar flow element (LFE) (CME, Davenport, IA) for flowrate measurement before being exhausted through a vacuum blower (Model 117416-00, Ametek, Paoli, PA). The air flowrate was controlled with a variable autotransformer (Staco Energy Products Co., Dayton, OH) that varied the voltage to the blower.

Pressures are measured just upstream of the cyclone entrance (P1), at the outlet skimmer pressure tap (P2), upstream of the LFE (P3), and across the LFE (P4). The pressures P1, P2, and P3 were measured with Magnehelic pressure gages (Dwyer, Michigan City, IN). The differential pressure across the LFE was measured with an inclined manometer (Dwyer, Michigan City, IN).

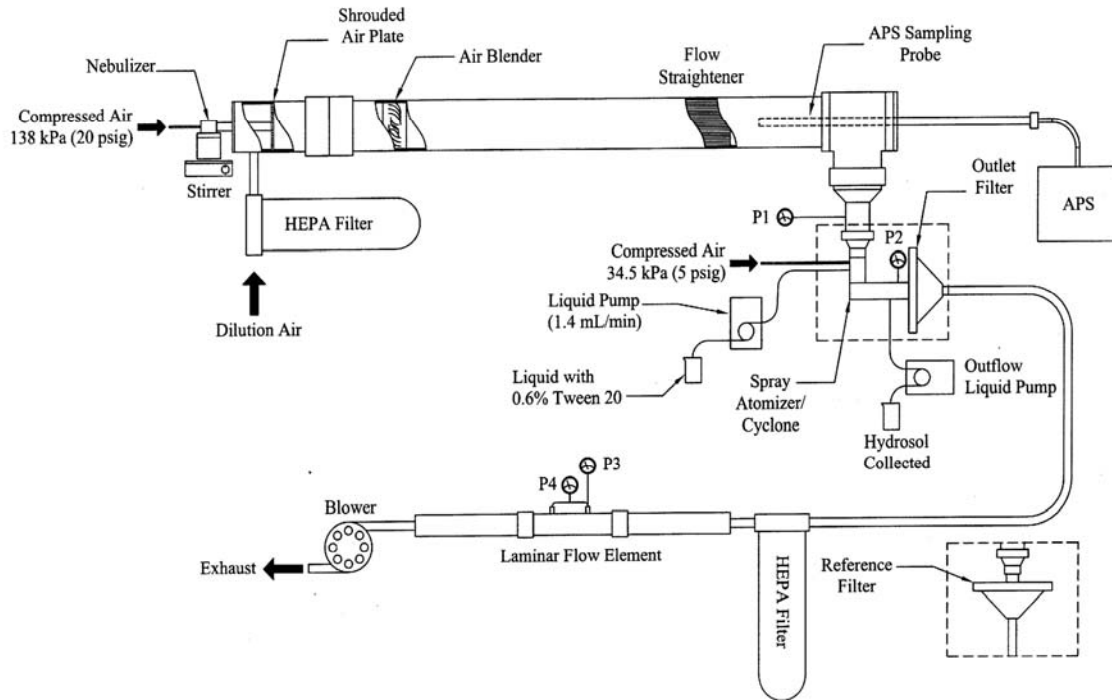


Figure 17. Schematic of test apparatus for aerosol performance evaluation of cyclones.

For each particle size and cyclone configuration, tests were conducted with the cyclone being operated five times in the flow and the reference filter used four times. A single test consisted of setting the air and liquid flowrates to the desired values, then sampling PSL with the cyclone and reference filter for a total of 40 minutes. At the completion of a test, the nebulizer was shut off but the output hydrosol continued to be collected for one more minute to clear the tubing.

The hydrosol samples were filtered through a 25 mm polycarbonate membrane filter (Isopore, Millipore, 0.6 μm DTPP). The filter was then placed in a jar containing

either 10 mL or 20 mL of ethyl acetate. The 203 mm x 254 mm glass fiber filters used for both the reference and outlet filters were soaked in 100 mL of ethyl acetate. Following each of the cyclone tests, the inside of the cyclone was thoroughly cleaned. Cotton-tipped applicators (Puritan Medical Products, Guilford, ME) were used to collect PSL deposited on the interior surface. The tips of the swabs were also soaked in 10 mL of ethyl acetate to elute the fluorescent tracer.

Each of the sample jars with hydrosol filters and recovery swab tips and the 203 mm x 254 mm glass fiber filter pans were sealed and weighed (Model VI-350, Acculab, Huntingdon Valley, PA, and Model AB104-S, Mettler Toledo, Columbus, OH), and then they were soaked overnight while being mixed by a rocking table (Rocker II Model 260350, Boekel Scientific, Feasterville, PA).

Prior to fluorometric analysis, each of the samples was weighed again to account for evaporation of the ethyl acetate. The volume of ethyl acetate used in computing the fluorescent concentration is defined by

$$V = V_{initial} - \frac{(m_{initial} - m_{final})}{\rho_{ethylacetate}} \quad [1]$$

where V is the volume of ethyl acetate to be used for fluorescent concentration calculations, $V_{initial}$ is the initial volume of ethyl acetate used to soak a filter, $m_{initial}$ is the initial weight of the sample prior to soaking overnight, m_{final} is the weight of the sample after soaking overnight, and $\rho_{ethylacetate}$ is the density of ethyl acetate.

Fluorometric analysis was performed using a Model FM109535, Quantech, Barnstead International fluorometer (Dubuque, IA). The concentration of each of the samples was found using

$$C = \frac{RV}{t} \quad [2]$$

C is the concentration, R is the average fluorometer reading adjusted for the background fluorescence, V is the volume of ethyl acetate, and t is the length of time during which the sample was collected.

The concentration of each of the 203 mm x 254 mm glass fiber reference filters is averaged together to give $C_{reference}$. The concentration of the hydrosol filters, $C_{hydrosol}$, the outlet filters, $C_{aerosol}$, and the recovery swab tips, $C_{wallloss}$, are then compared with the reference concentration to give the aerosol-to-hydrosol collection efficiency (η_{AH}), aerosol-to-aerosol collection efficiency (η_{AA}), and percent wall loss (WL), respectively.

$$\eta_{AH} = \frac{C_{hydrosol}}{C_{reference}} \quad [3]$$

$$\eta_{AA} = 1 - \frac{C_{aerosol}}{C_{reference}} \quad [4]$$

$$WL = \frac{C_{wallloss}}{C_{reference}} \quad [5]$$

Plots were made for the aerosol-to-hydrosol and aerosol-to-aerosol collection efficiencies as a function of the particle size.

Time Response of the Cyclone

Once the cyclone is challenged with an aerosol, it is desired to know how long it takes for the cyclone to collect and aspirate the hydrosol. The AAC with the hydrophobic coating on the outlet skimmer, the White-type cyclone (ca. 2003), and the shortened acrylic AAC were evaluated for time response.

The same test apparatus used for the aerosol-to-hydrosol transfer tests described previously was used for this experiment. The outlet filter was removed for these experiments. The testing procedures follow.

The air flowrate and liquid flowrate were set to their respective values of 780 L/min and 1.4 mL/min. Two micrometer polystyrene latex spheres (PSL) (Duke Scientific, Palo Alto, CA) were used in this evaluation. Five one-minute samples were collected in sealable, glass sample jars. (Clean empty sample jars were weighed prior to testing.) The nebulizer was then turned on. Ten more 1-minute samples were collected followed by five 2-minute samples, four 3-minute samples, and two 4-minute samples. The nebulizer was then turned off and five more 1-minute samples were collected. Each of the sample jars were then weighed to measure the amount of water collected over each time interval.

The ethyl acetate in the samples was allowed to evaporate so that only the PSL remained. Once evaporated, 4 mL of ethyl acetate was added to each jar. The jars were sealed and weighed again, and allowed to soak over night.

Reference 203 mm x 254 mm glass fiber filters (Type A/E, Pall, East Hills, NY) were taken between each of the cyclone tests. They were run for 5 minutes with no PSL present, 40 minutes with aerosolized PSL, and another five minutes with the nebulizer turned off. The reference filters were placed in 100 mL of ethyl acetate, sealed in pans, weighed, and also soaked overnight. While soaking overnight, the sample jars and filter pans were placed on rocking tables (Boekel Scientific, Feasterville, PA) to promote mixing.

Prior to fluorometric analysis, each of the sample jars and filter pans were again weighed to account for loss of ethyl acetate due to evaporation. The volume of ethyl acetate used in the analysis of the concentration of fluorescence was again determined by Equation [1]. Fluorometric analysis was performed and the concentration of each of the samples was found using Equation [2].

The concentration of the samples was corrected to reflect the amount of water that was collected each minute, as this value was not steady. The amount of water was found from weighing the jars as the samples were collected. These values were then normalized with the average liquid flowrate.

$$F_{water} = \frac{V_{water_i}}{\bar{V}_{water}} \quad [6]$$

F_{water} is the normalized volume of water collected for each sample, V_{water} is the volume of water collected for each sample period, and \bar{V}_{water} is the average volume of water collected per minute.

The corrected concentration ($C_{corrected}$) for each sample was then the result of dividing by the normalized water correction factor.

$$C_{corrected} = \frac{C}{F_{water}} \quad [7]$$

Once the concentration of each of the samples and reference filters was determined, the samples were compared individually to the average value of the concentration of the reference filters to find the aerosol-to-hydrosol collection efficiency of the cyclone at each time, η_{AH} .

$$\eta_{AH} = \frac{C_{corrected}}{C_{reference}} \quad [8]$$

A plot of the aerosol-to-hydrosol collection efficiency as a function of time was then constructed in order to determine the time constant of the initial response and final decay of the cyclones.

For the initial response of the system, the fraction of the full scale (F) for each sample was first found according to

$$F = \frac{\eta_{AH}}{\bar{\eta}_{AH}} \quad [9]$$

where $\bar{\eta}_{AH}$ is the average aerosol-to-hydrosol collection efficiency over all of the samples near the full scale collection capability of the cyclone.

For each test of a cyclone, the first five samples following the start of the PSL flow (samples 6 through 10) were used to evaluate the initial response. These values were then averaged together and a curve was fit using Microsoft Excel. The equation for this curve is

$$F = 1 - \frac{1}{1 + At^B} \quad [10]$$

where the constants A and B are found by optimizing the curve fit. The time at which 63% of the full scale collection efficiency is realized (t) can then be calculated using Equation [10] and the values of A and B . The time response of each of the cyclones was corrected for the range of collection efficiency by multiplying by the instantaneous aerosol-to-hydrosol collection efficiency at each time interval.

The time constant for the decay of the cyclone once the aerosol challenge was removed was found using

$$F = \frac{1}{1 + At^B} \quad [11]$$

and the same techniques for the initial response were followed.

Power Consumption of the Cyclone

Power consumption aspects of three cyclones and three blowers were compared. Two White-type cyclones (ca. 2003 and 1999), one from the stand-alone unit and one from a third test unit were used. A Tangential Transpirated Wall Cyclone (TTWC) was also evaluated for comparison. A blower included with the third test unit (Model 119104, Ametek, Paoli, PA) and two blowers selected by the lab (Models 116634 and 117418, Ametek, Paoli, PA) were used to setup the airflow. A nominal air flowrate of

780 L/min was used. This air flowrate was pre-determined by the White-type cyclone system.

The air flowrate was varied over a range of $\pm 20\%$, and power and pressure measurements will be recorded for each cyclone and blower combination. Plots of “Power Consumption vs. Air Flowrate” and “Pressure Drop vs. Air Flowrate” were generated.

The experimental apparatus used to test the power requirements of the cyclones is shown in Figure 18. Air entered the setup and passed through a laminar flow element (LFE) (CME, Davenport, IA). The air then passed through the cyclone to a section of pipe containing an optional flow straightener. This flow straightener consisted of two cross pieces made of thin, flat plates. The static pressure at the outlet of the cyclone was measured with this flow straightener in place. The flow straightener was removed for the power measurements to eliminate the load produced by the flow straightener. The blower used for testing then exhausted this air into a plenum where the pressure is matched to the inlet condition. A second blower was used to accomplish this.

Several pressure measurements were taken across the system including the upstream gage pressure to the LFE (P1), and the differential pressure across the LFE (P2). The value of P2 was then used to determine the air flowrate through the LFE based on the calibration data provided by the manufacturer as corrected for the value of P1. The inlet gage pressure to the inlet of the cyclone was measured at P3. The pressure drop across the cyclone, with the flow straightener in place, was measured at P4 and the pressure drop across the cyclone without the flow straightener in place (P5). The pressure drop P5 is the same measurement taken by the White-type cyclones for setting the air flowrate. The differential pressure between the inlet to the cyclone and the exhaust of the tested blower was measured at P6, which should be equal to zero. All of the pressure gages used were calibrated and checked against a digital manometer (Series 2177-2, Dwyer, Michigan City, IN) for accuracy. Thermocouples were used to measure the ambient room temperature, T1, and the air temperature entering the cyclone, T2.

Power measurements, including power factor, voltage, and current, were recorded using a power meter (Fluke 39, SN 6589017). This was connected to the wiring harness of the blower.

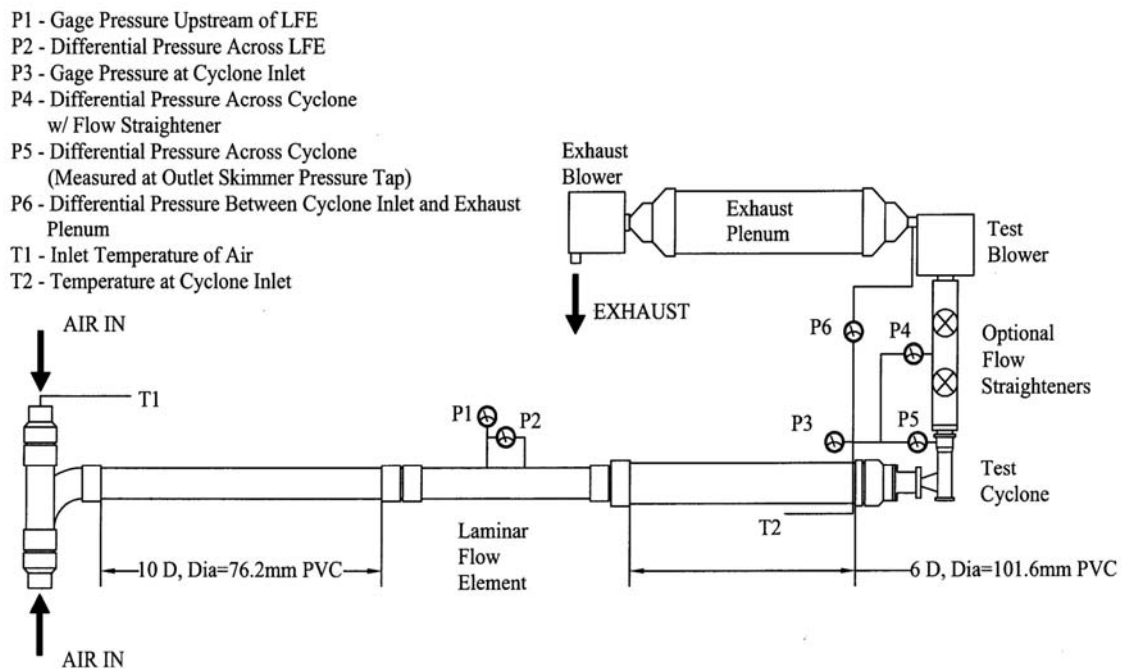


Figure 18. Schematic of test apparatus for power consumption test.

Prior to testing, the entire section of the test setup was leak-checked to hold a vacuum. For each cyclone blower combination, the air flowrate was adjusted using the potentiometer included with the blower's electronics. Air flowrates, ranging from approximately 780 L/min \pm 20% were set. The pressures, temperatures, and power

readings were then recorded. This series of tests was run both with and without the flow straightener in place.

The air flowrate, Q , was calculated using P_2 and the LFE manufacturer's calibration. The standard air flowrate, Q_{standard} , was then calculated using the following equation, correcting for pressure and temperature.

$$Q_{\text{standard}} = \frac{Q(P_{\text{std}} - P_1)}{P_{\text{std}} \left(\frac{T_{\text{std}}}{T_1} \right)} \quad [12]$$

The ideal power is calculated as follows, where ΔP_{4-6} is the pressure drop across the blower.

$$Power_{\text{ideal}} = Q\Delta P_{4-6} \quad [13]$$

The efficiency of the blower is then found to be:

$$\eta = \frac{Power_{\text{ideal}}}{Power} \quad [14]$$

RESULTS AND DISCUSSION

Aerosol-to-Hydrosol and Aerosol-to-Aerosol Performance

Although over the course of this study, many cyclones were tested for their aerosol performance, only the most successful and promising for further study are reported. The AAC was tested with two different outlet skimmers, an uncoated aluminum outlet skimmer and an outlet skimmer with a hydrophobic coating. A shortened version of the AAC, made from acrylic, and the White-type cyclone (ca. 2003) were also evaluated. The aerosol-to-hydrosol performances for the four cyclone configurations are shown below.

Figure 19 shows the aerosol-to-hydrosol collection efficiency for the White-type cyclone. The error bars represent one standard deviation. Blue squares depict data points in which there was no water carryover from the outlet skimmer. The large range on error bars is primarily due to the affects of the water carryover.

The aerosol-to-aerosol collection efficiency of the White-type cyclone is pictured in Figure 20. The large standard deviations are due to hydrosol carryover which carries PSL out of the cyclone and impacts onto the outlet filter. Runs in which there was no carryover show good aerosol-to-aerosol collection efficiency with a cut-point at approximately $0.9 \mu\text{m}$.

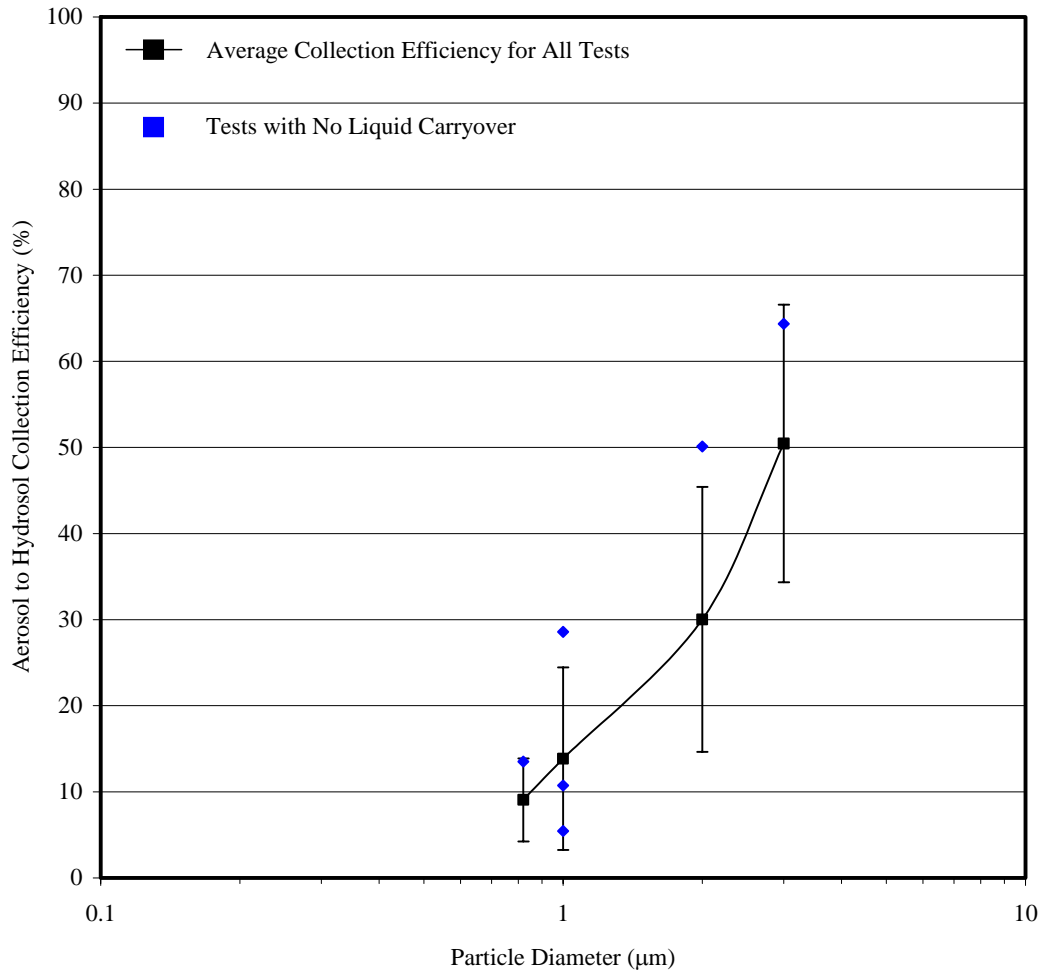


Figure 19. Aerosol-to-hydrosol collection efficiency of the White-type cyclone (ca. 2003).

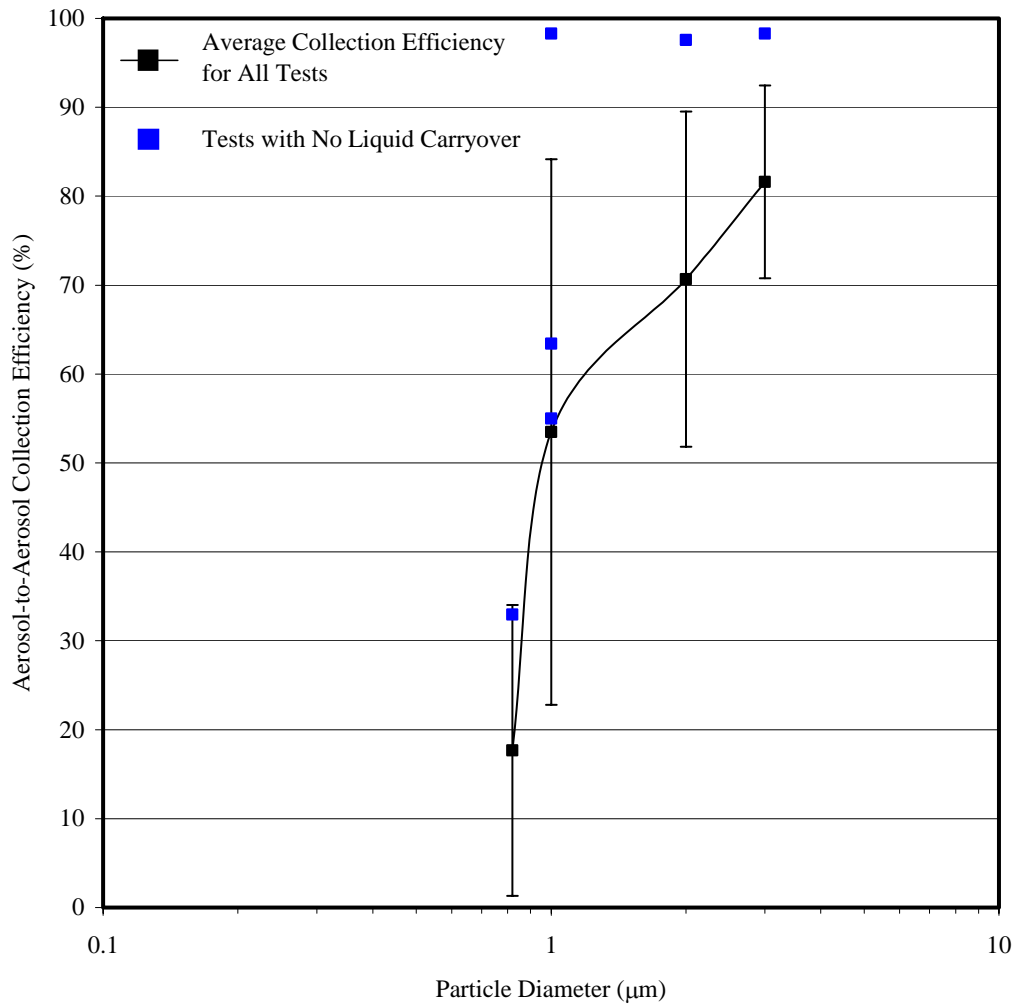


Figure 20. Aerosol-to-aerosol collection efficiency of the White-type cyclone (ca. 2003).

The AAC was run with an uncoated and coated skimmer. Figures 21 through 24 show the aerosol-to-hydrosol and the aerosol-to-aerosol collection efficiencies of the two configurations. The standard deviations were smaller than those for the White-type cyclone, and the liquid carryover problems were not as prevalent. The cut-point of the cyclone was approximately 1.6 μm for aerosol-to-hydrosol collection and 1 μm for aerosol-to-aerosol collection.

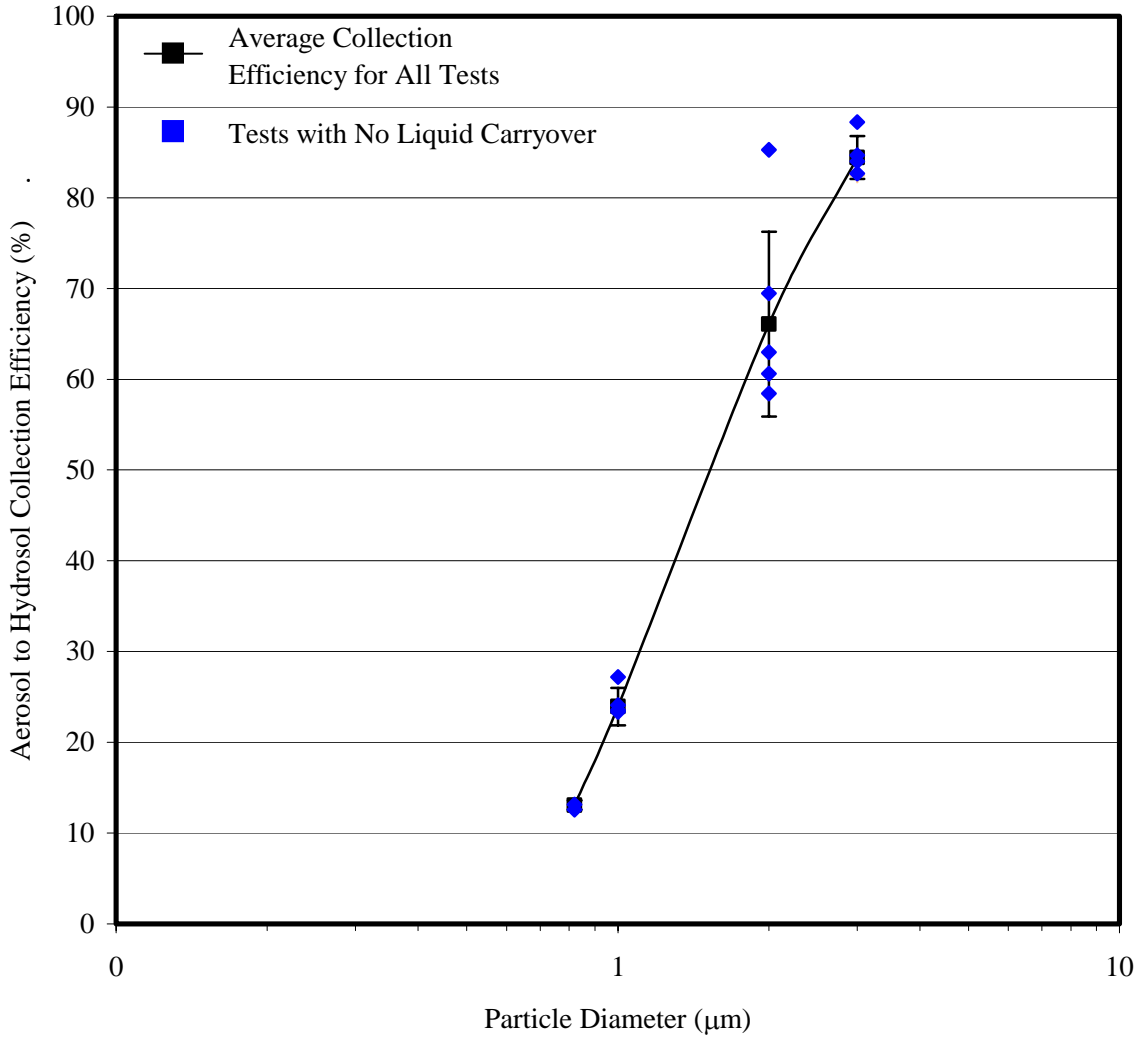


Figure 21. Aerosol-to-hydrosol collection efficiency of AAC with aluminum outlet skimmer.

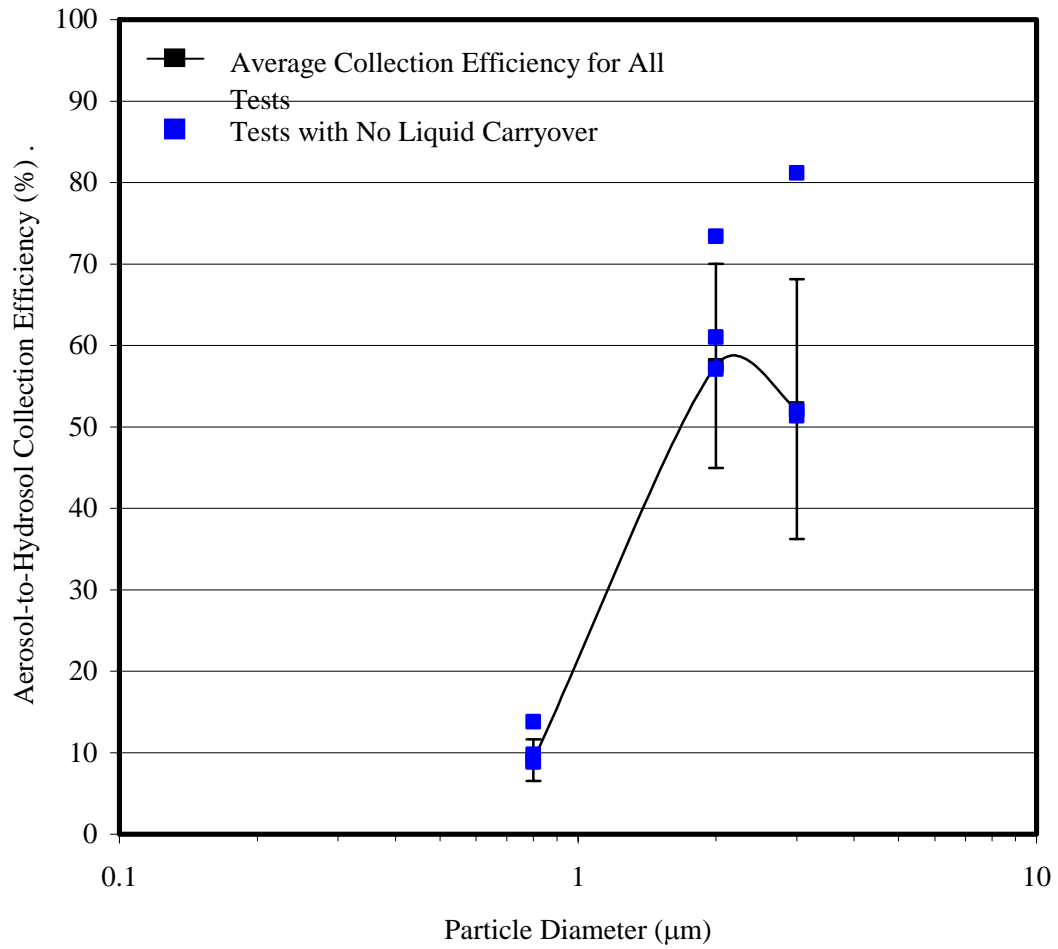


Figure 22. Aerosol-to-hydrosol collection efficiency of AAC with coated, hydrophobic outlet skimmer.

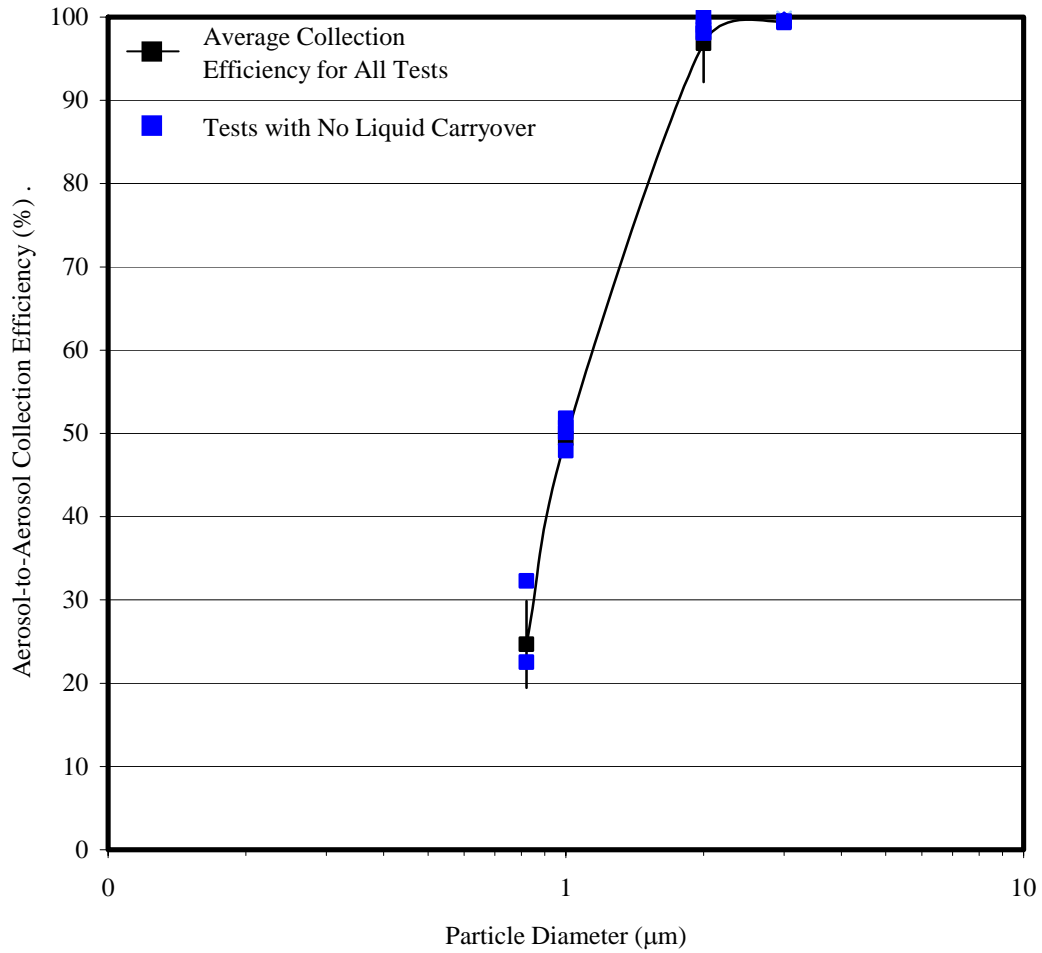


Figure 23. Aerosol-to-aerosol collection efficiency of AAC with aluminum outlet skimmer.

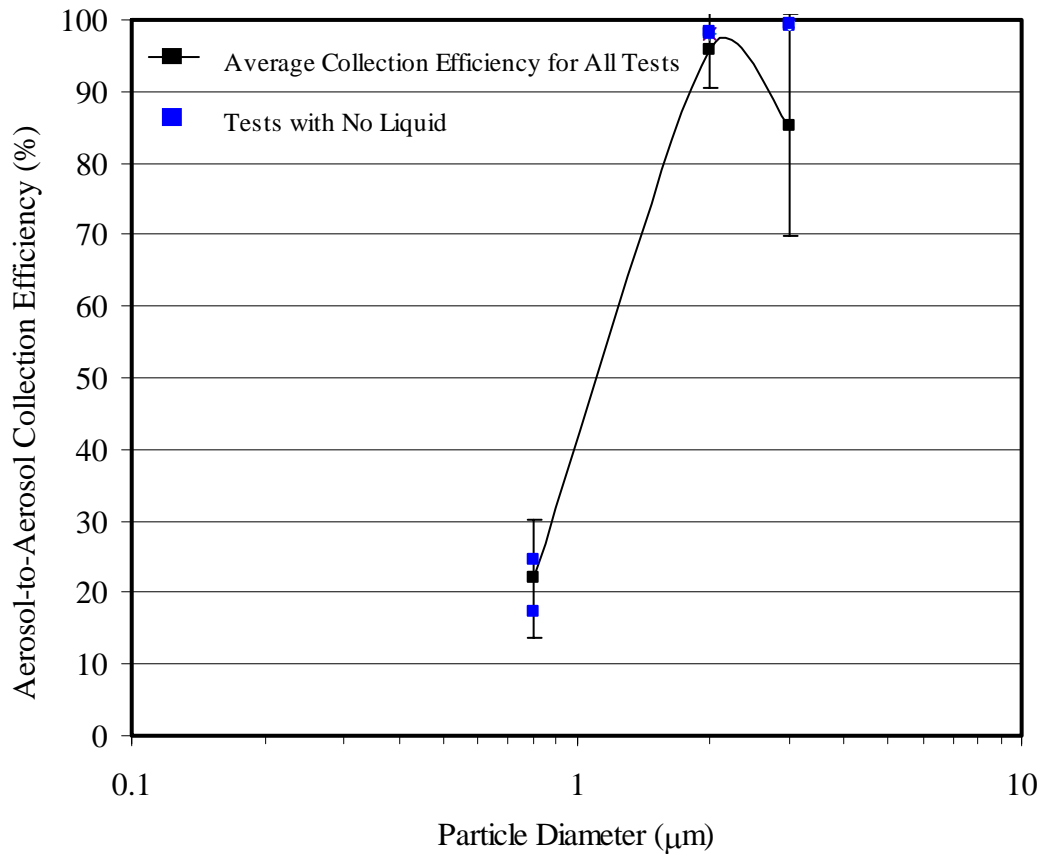


Figure 24. Aerosol-to-aerosol collection efficiency of AAC with coated, hydrophobic outlet skimmer.

The outlet skimmer with the hydrophobic coating tended to have more problems with carryover than did the uncoated aluminum skimmer. On many of the runs with the coated skimmer, the wall losses jumped as much as 20%. On other cyclone configurations, the White-type and the AAC with uncoated skimmer, the wall losses were approximately 5%. These wall loss values were taken from the 3 μm tests. Further wall loss data is contained within the Appendix.

The shortened acrylic version of the AAC was run to find the aerosol-to-hydrosol collection efficiency. The efficiency results are shown in Figure 25.

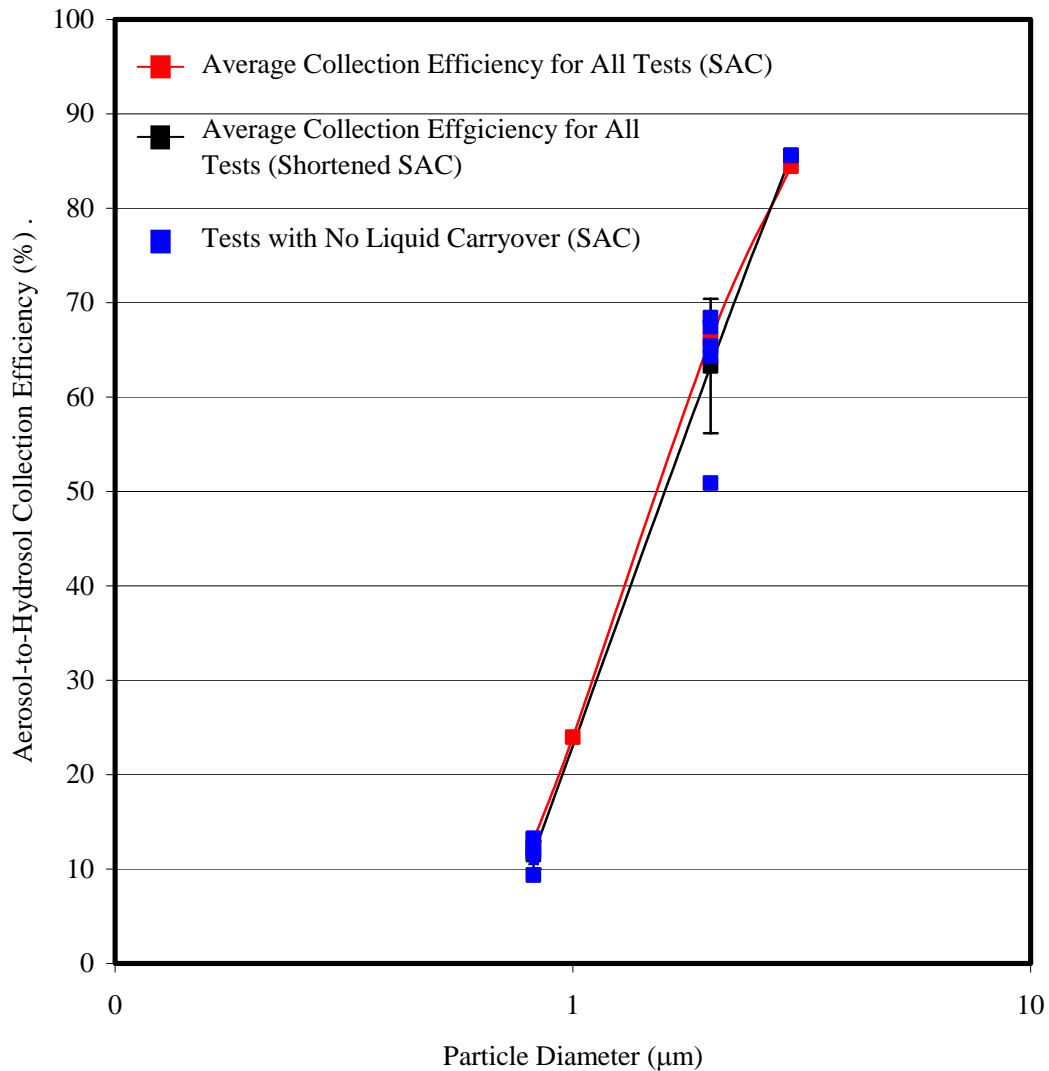


Figure 25. Aerosol-to-hydrosol collection efficiency of shortened AAC with grooved outlet skimmer.

There were very few problems with liquid carryover in this cyclone configuration. The outlet skimmer was replaced with the grooved skimmer shown previously in Figure 13 after it was determined that the other skimmers would not work

with this configuration due to hydrosol carryover. The results show a similar aerosol-to-hydrosol collection efficiency at 0.82, 2, and 3 μm compared with the AAC.

Time Response of the Cyclone

Time response tests were run for the White-type cyclone (ca. 2003), AAC, and the shortened AAC. The results for the White-type cyclone are presented in Figure 26. The time response to recognize a challenge was found to be 3 minutes, and the time decay to clear the cyclone of material is 1.1 minutes. These values were found from two tests which did not have problems with liquid carryover. After including three tests which did have liquid carryover, the time response increases to 8 minutes.

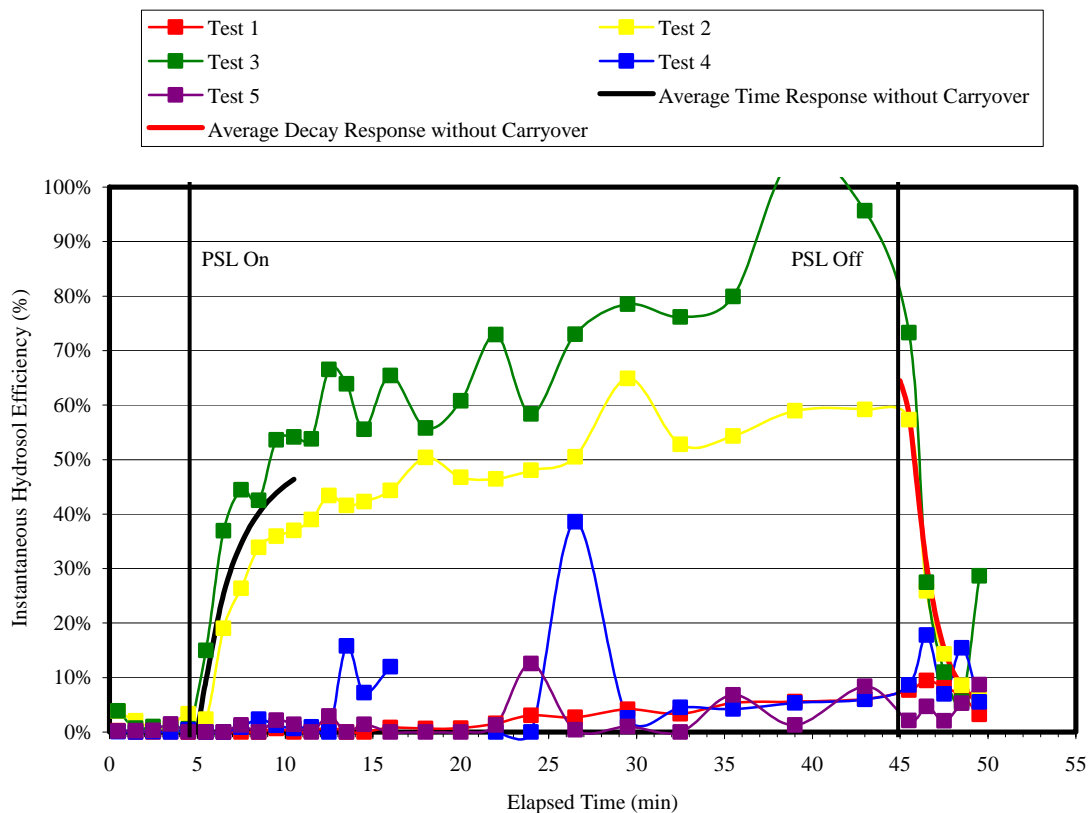


Figure 26. Time response of the White-type cyclone (ca. 2003).

The results for the AAC with the skimmer with the hydrophobic coating are shown in Figure 27 below. The time constant to recognize a signal was found to be 2.75 minutes, and the time constant for the cyclone to clear itself once a challenge is no longer present is 2.5 minutes.

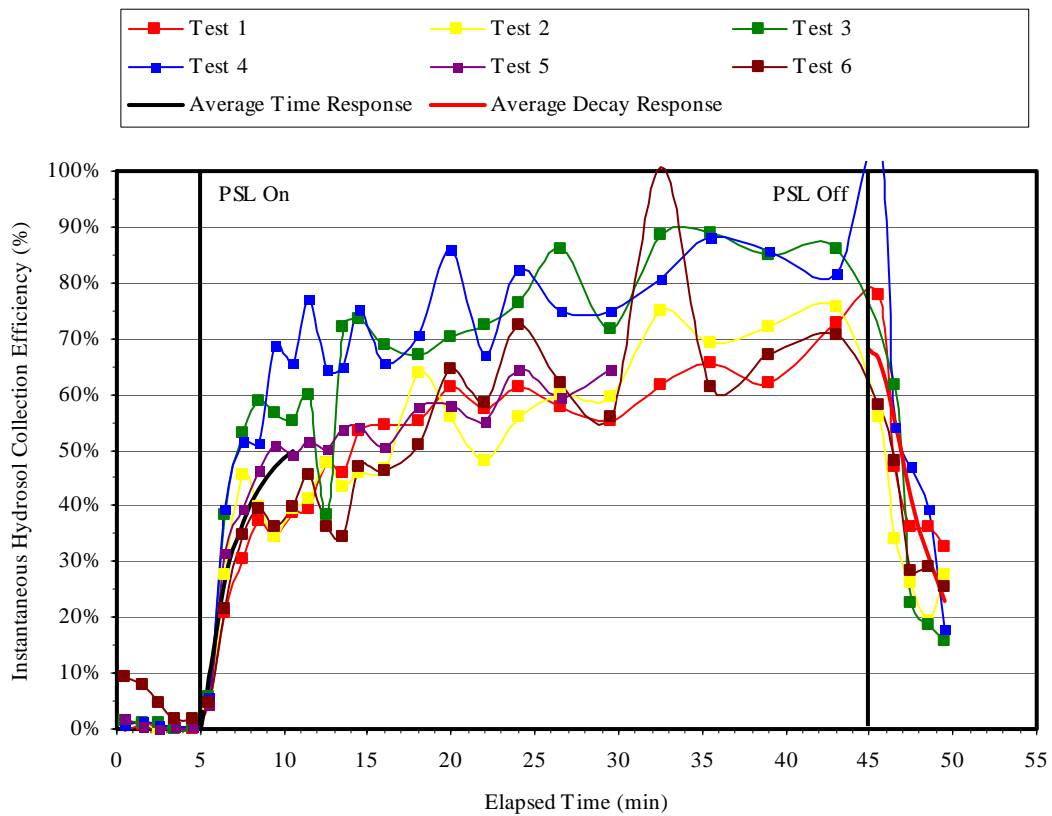


Figure 27. Time response of AAC with hydrophobic coating on outlet skimmer.

The shortened acrylic AAC was run with the grooved outlet skimmer. The time response to recognize the presence of a challenge is 1.5 minutes. The response time for the decay of the signal is 1.25 minutes. These results are shown in Figure 28.

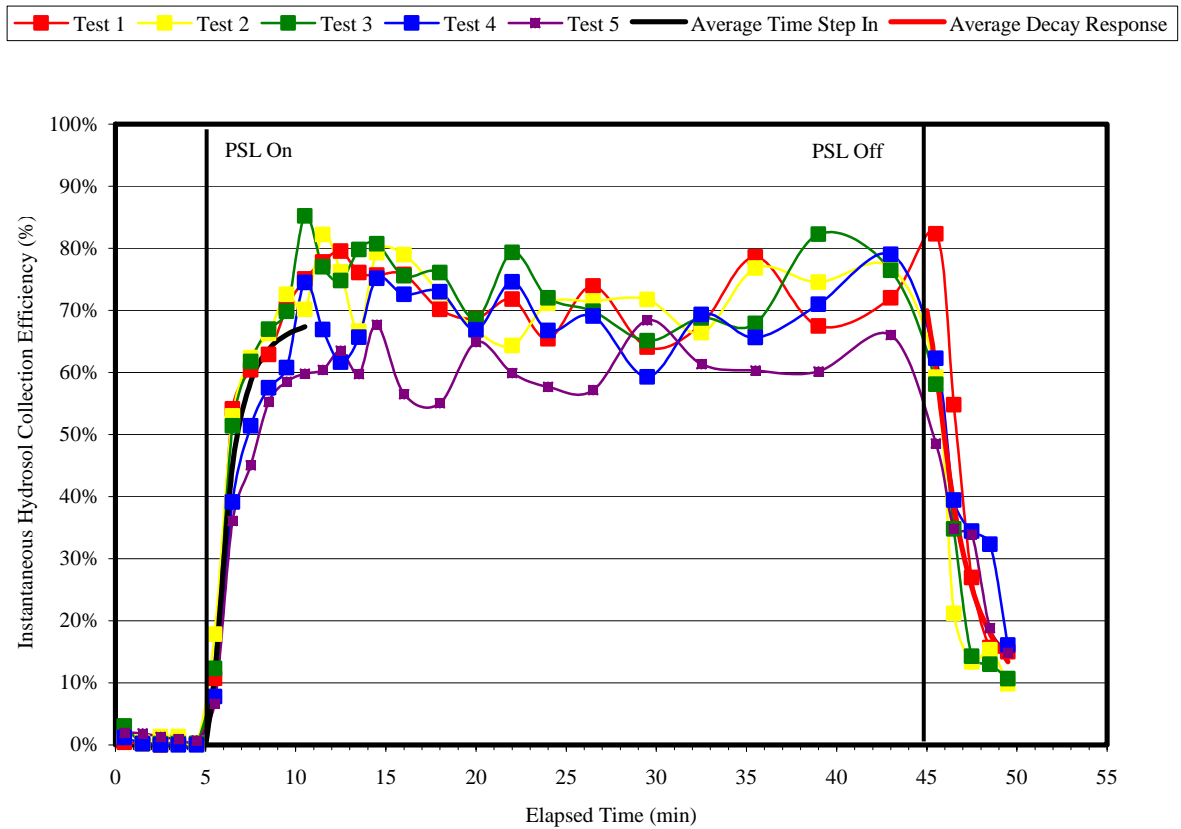


Figure 28: Time response of shortened AAC with grooved outlet skimmer.

Power Consumption of the Cyclone

The power consumption of each blower combined with each cyclone was recorded for various flowrates. The two 9- and 8-amp blowers (Ametek models 117418 and 119104, respectively) follow a similar trend, but the 4-amp blower (Ametek model 116634) tends to provide a higher flowrate at an equivalent power. However, the Model 116634 is unable to reach as high of an air flowrate, and does not reach the 780 L/min mark for the White-type cyclone (ca. 1999) pairing. Each of the three cyclones also affects the power consumption, based on its pressure drop. A plot is shown in Figure 29.

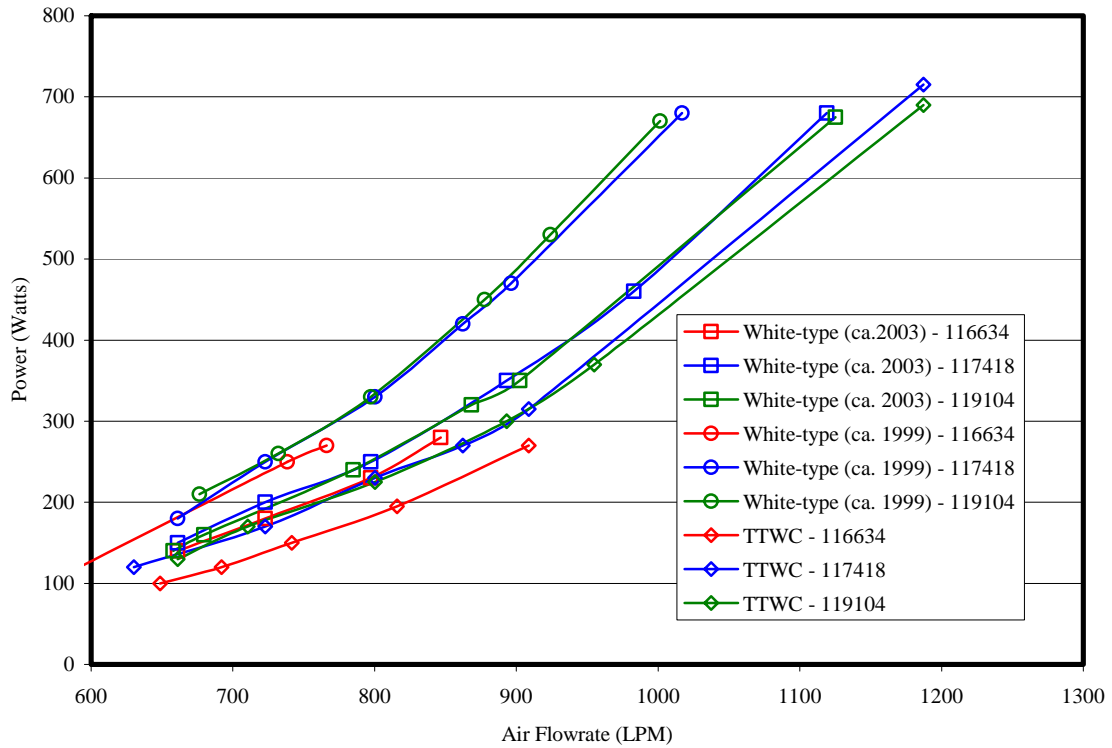


Figure 29. Power consumption vs. air flowrate through wetted wall cyclones using blower models 116634, 117418, and 119104. (Power measurements taken without flow straightener.)

The pressure drop across each cyclone is shown in Figure 30. Although the values for each blower are shown, the pressure drop is independent of the blower used. It is obvious that each cyclone has its own curve. For an air flowrate of 780 L/min, the three cyclones have varying differential pressure measurements: 6.2 kPa (25 inches of H₂O) for the White-type cyclone (ca. 1999), 4.5 kPa (18 inches of H₂O) for the White-type cyclone (ca. 2003), and 4 kPa (16 inches of H₂O) for the TTWC.

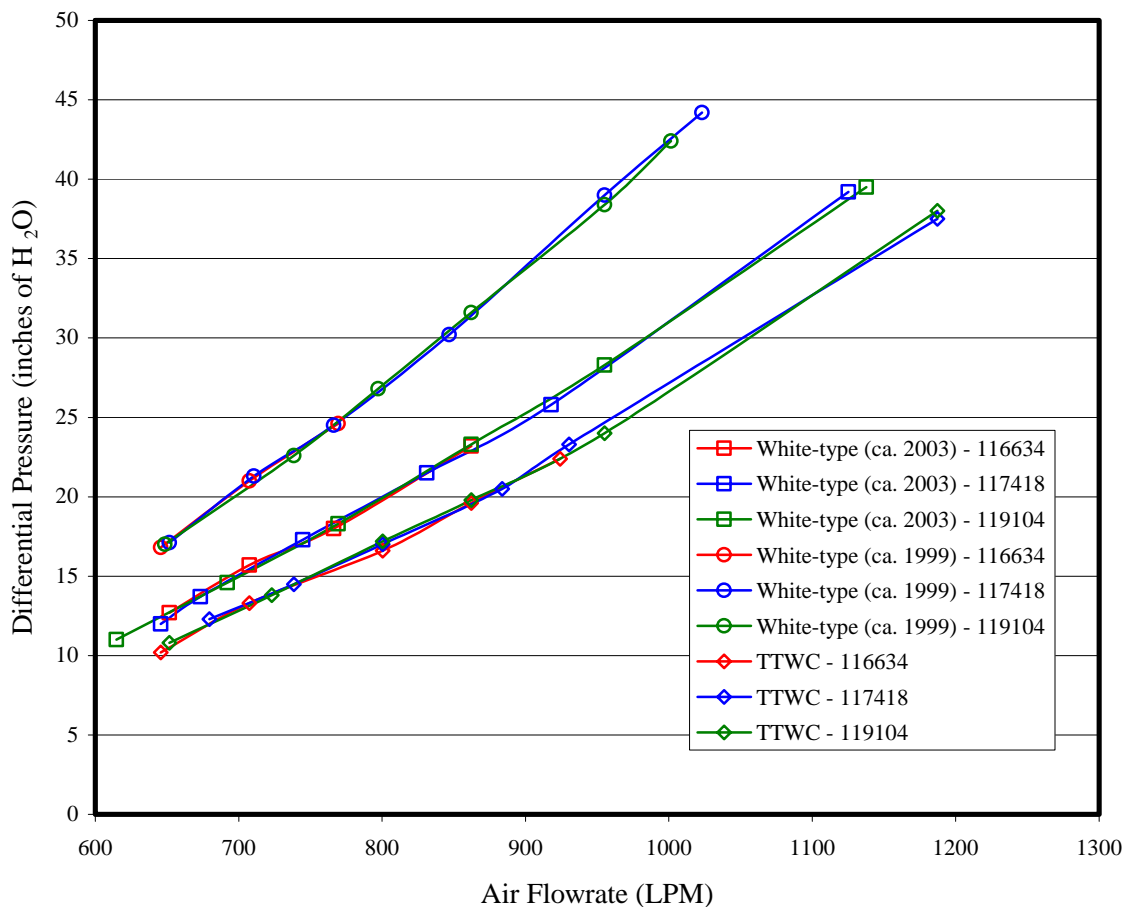


Figure 30. Differential pressure across cyclones with flow straightener in place using blower models 11634, 117418, and 119104. (Pressure measurements taken with flow straightener.)

The White-type cyclone currently in use measures the air flowrate based on the differential pressure across the cyclone measured at the outlet skimmer pressure tap. Figure 31 shows the pressure readings taken at this point for various air flowrates for each of the cyclones. The air flow straightener was not in place for these measurements. Measuring air flowrate based on an outlet pressure of 6.2 kPa (25 inches of H₂O) results in different values: 780 LPM for White-type (ca. 1999), 930 LPM for the White-type (ca. 2003), and 1000 LPM for the TTWC.

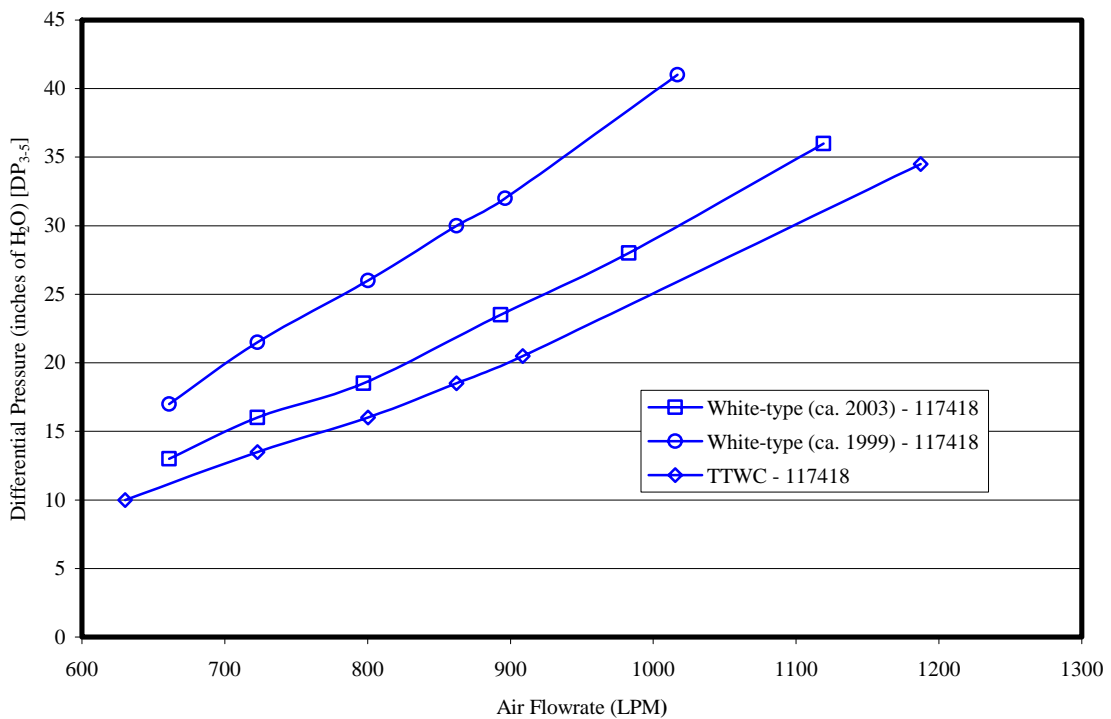


Figure 31. Comparison of differential pressure measurements taken on each cyclone at the outlet skimmer pressure tap.

SUMMARY AND CONCLUSIONS

Aerosol-to-Hydrosol and Aerosol-to-Aerosol Performance

The White-type cyclone (ca. 2003) was found to have liquid carryover problems that inhibit its ability to consistently deliver a sample. The aerosol-to-aerosol transmission cut-point was found to be $0.9\ \mu\text{m}$ and the aerosol-to-hydrosol collection efficiency cut-point is $3.0\ \mu\text{m}$ with the effects of liquid carryover considered. The data provided by White et al. should be considered under “ideal” conditions with no hydrosol carryover. The manufacturer’s aerosol-to-aerosol cut-point was measured with no liquid flow.

The introduction of liquid through spray atomization provides a better aerosol-to-hydrosol transfer efficiency due to a more effective wetting of the main aerosol impaction area of the cyclone wall just below the cyclone inlet. The aerosol-to-hydrosol collection efficiency cut-point was found to be near $1.6\ \mu\text{m}$, and the aerosol-to-aerosol cut-point is $1.0\ \mu\text{m}$. Unfortunately, PSL sizes between 1 and $2\ \mu\text{m}$ were not readily available to better verify the cut-point of this cyclone. The collection efficiency of this configuration at $3\ \mu\text{m}$ was found to be 85% compared with 50% for the White-type cyclone. This result was for the uncoated skimmer.

The outlet skimmer with the hydrophobic coating proved to be not as efficient, with respect to aerosol-to-hydrosol transfer and aerosol-to-aerosol transmission with cut-points of 1.7 and $1.2\ \mu\text{m}$, respectively. This shows the effects a subtle change can make on this device. The collection efficiency of this configuration at $3\ \mu\text{m}$ was found to be 85% compared again with 50% for the White-type cyclone.

The short AAC provides a comparable aerosol-to-hydrosol collection efficiency with that of the AAC. At $2\ \mu\text{m}$, it has a comparable aerosol-to-hydrosol collection efficiency to the AAC with a value of 65%, and it did perform better and more consistently than the White-type cyclone at this size.

Time Response of the Cyclone

The time response of the White-type cyclone (ca. 2003) was shown to be 3 minutes. Liquid carryover increases the time response to 8 minutes. The decay response for no liquid carryover is 1.1 minutes. The AAC, having similar internal dimensions, has an initial response of 2.75 minutes and a decay response of 2.5 minutes.

The shortened AAC proved to reduce the initial time response of the cyclone by approximately 50%. The initial response time is 1.5 minutes, and the decay response is 1.25 minutes.

Power Consumption of the Cyclone

The type of blower selected affects the power consumption, and different cyclones have different pressure drops, which also affects the power. Although the TTWC has a different inlet configuration, the two White-type cyclones should have a similar inlet profile. However, after recording different pressure drops, it was found that their inlet areas had slightly different dimensions. This may be an effect of machining during production. Multiple cyclones from the manufacturer should be tested before drawing any other conclusions.

From these results, the Ametek Blower model 116634 paired with the TTWC cyclone would have the least power consumption at 780 L/min. A power saving of 27% over the White-type (ca. 2003) with the 119104 blower and 44% over the second White-type (ca. 1999) with the 119104 blower were realized. This test was limited to only three blower models produced by one manufacturer. A search for different blower makes and models is recommended. The electrical discharge machined (EDM) inlet on the TTWC produces a favorable improvement on the pressure drop reduction across the cyclone.

Final Remarks

In conclusion, a variation of the current White-type cyclone design consisting of an airblast atomizer placed upstream of a reconfigured inlet profile was presented. It

provides both a better aerosol-to-hydrosol collection efficiency across a range of particle sizes as well as reduces the pressure drop across the cyclone thereby reducing the power requirements of the system.

RECOMMENDATIONS FOR FUTURE WORK

An alternative method for recovering particles in the form of a hydrosol was presented. Throughout the testing process, problems with carryover of hydrosol bypassing the outlet skimmer were prevalent with all cyclones. Both of the White-type cyclones received had signs of carryover evidenced by corrosion around the cyclone-blower interface. Under laboratory conditions, in which the ambient temperature was maintained at 72°F, and the cyclone was fixed in a level position, however, these problems persisted. Prior to every test, each cyclone was cleaned and free of any debris or contamination, and the ambient air flow was passed through a HEPA filter. It was found that fibers and debris tended to “short circuit” the hydrosol past the skimmer. More development is needed to solve the hydrosol bypass issue. Testing must then be done that would reflect field conditions; i.e. changing temperatures, rough motions, and inclinations.

A new blower should be selected or designed to reduce the power consumption of the system. We chose available, off-the-shelf, blowers from one company, but there may be more suitable options.

REFERENCES

- John, S.F., Hillier, V.F., Handley, P.S., and Derrick, M.R. (1995). Adhesion of *Staphylococci* to Polyurethane and Hydrogel-coated Polyurethane Catheters Assayed by an Improved Radiolabelling Technique, *J. Med. Microbiology*, 43:133-140.
- Lefebvre, A.H. (1989). *Atomization and Sprays*, Hemisphere Publishing Corporation, New York.
- May, K.R. (1973). The Collison Nebulizer. Description, Performance & Application. *J. Aerosol Sci.* 4:235-243.
- Richardson, M. (2003). A System for Continuous Sampling of Bioaerosols Generated by a Postal Sorting Machine. M.S. Thesis, Texas A&M University, College Station TX.
- Sioutas, C., Koutrakis, P. and Burton, R.M. (1994). Development of a Low Cutpoint Slit Virtual Impactor for Sampling Ambient Fine Particles. *J. Aerosol Sci.* 25(7):1321-1330.
- White, L.A., Hadley, D.J., Davids, D.E., and Naylor, R. (1975). Improved Large Volume Sampler for the Collection of Bacterial Cells from Aerosol. *Appl. Microbiol.* 29(3):335-339.
- Willeke, K., Lin, X., and Grinshpun, S.A. (1998). Evaluation of a High Volume Aerosol Concentrator, *Aerosol Sci. Technol.* 28:439-456.

APPENDIX

Table 1. Aerosol-to-hydrosol collection efficiencies of cyclones. Green blocks indicate no liquid carryover for that individual test.

	Particle Size (Diameter)			
	(μm)			
	0.82	1.0	2.0	3.0
White-type (ca. 2003)	11.86	26.19	50.19	44.74
	12.29	14.76	11.87	25.26
	3.3	3.84	41.34	62.79
	4.42	23.94	23.94	55.59
	13.57	24.32	23.15	64.53
AAC				
Aluminum Uncoated Outlet	12.61	21.56	85.4	84.9
	12.84	24.13	69.61	84.2
	13.82	27.24	59.92	88.46
	13.16	23.4	60.72	82.6
		23.58	58.55	82.87
			63.02	
Aluminum Coated Outlet	8.21		57.43	32.91
	13.78		57.1	51.18
	9.79		38.49	44.53
	6.59		61.02	51.37
	7.31		73.41	81.18
	8.86			51.99
Shortened AAC	9.35		64.35	67.83
	10.95		67.47	84.05
	12.22		50.89	84.7
	11.8		65.38	79.18
	13.26		68.39	85.58

Table 2. Aerosol-to-aerosol collection efficiencies of cyclones. Green blocks indicate no liquid carryover for that individual test.

	Particle Size (Diameter)			
	(μm)			
	0.82	1.0	2.0	3.0
White-type (ca. 2003)	70.32	44.98	2.46	22.4
	75.39	68.65	52.71	28.08
	105.04	80.67	22.07	13.73
	93.59	36.55	39.88	26.1
	66.86	1.71	30.1	1.7
AAC				
Aluminum Uncoated Outlet	67.7	53.42	0	0.17
	79.36	49.84	1.05	0.25
	76.53	49.19	12.52	0.66
	77.59	52.08	1.94	0.49
		48.18	1.87	0.81
			1.5	
Aluminum Coated Outlet	88.86		1.88	27.16
	82.69		1.78	28.39
	75.53		13.82	30.91
	82.64		1.97	0.71
	71.94		1.97	0.45
	66.54			0.53

Table 3. Recovered wall losses from cyclones. Green blocks indicate no liquid carryover for that individual test.

	Particle Size (Diameter)			
	(μm)			
	0.82	1.0	2.0	3.0
White-type (ca. 2003)	4.6	15.69	17.97	18.08
	5.78	11.81	16.56	12.69
	4.94	12.99	12.28	2.38
	4.6	12.6	8.63	5.42
	5.46	9.61	20.58	2.05
AAC	5.17	10.02	4.11	5.92
Aluminum Uncoated Outlet	3.83	12.43	14.99	5.94
	4.71	7.93	9.32	5.65
	4.75	12.36	23.67	4.09
		13.96	17.61	2.76
			18	
Aluminum Coated Outlet	2.91		22.28	24.3
	2.82		15.67	2.45
	7.32		21.81	3.36
	5.89		16.37	20.09
	7.15		5.36	2.01
	5.43			22.21
Shortened AAC	3.21		7.36	2.98
	5.62		1.53	4.79
	4.9		5.39	5.38
	4.39		5.31	3.32
	4.65		4.31	0.96

Table 4. Time response of cyclones.

	Time Response	Decay Response	Time Response	Decay Response
	(sec)	(sec)	(sec)	(sec)
White-type (ca. 2003) (No Liquid Carryover)	171	67	2.85	1.12
White-type (ca. 2003) (with Liquid Carryover)	476		7.93	
AAC	163	144	2.72	2.40
Shortened AAC	88	73	1.47	1.22

VITA

Name: Brandon Wayne Moncla

Date and Place of Birth: 08/30/1978
Beaumont, Texas

Permanent Address: 835 Nantucket
Beaumont, TX 77706

Education: M.S. Mechanical Engineering (August 2004)
Texas A&M University
College Station, TX 77843

B.S. Mechanical Engineering (December 2002)
Texas A&M University
College Station, TX 77843

Work Experience: 1/03-present Graduate Research Assistant
Aerosol Technology Laboratory
Mechanical Engineering Department
Texas A&M University
College Station, TX 77843

9/01-12/02 Undergraduate Research Assistant
Aerosol Technology Laboratory
Mechanical Engineering Department
Texas A&M University
College Station, TX 77843

6/2000-8/2001 Student Intern
Summers Manufacturing Solutions, Inc.
PMB 786
Beaumont, TX 77706